Active Disturbance Rejection Control for Load Frequency Control of Bangladesh Power System

by

A. H. M. Sayem

A Thesis Submitted to the Department of Electrical and Electronic Engineering of Bangladesh University of Engineering and Technology in Partial Fulfillment of the Requirement for the Degree of

Master of Science in Electrical and Electronic Engineering

Department of Electrical and Electronic Engineering

BANGLADESH UNIVERSITY OF ENGINEERING AND TECHNOLOGY

Dhaka-1000, Bangladesh

November, 2012

The thesis titled **"Active Disturbance Rejection Control for Load Frequency Control of Bangladesh Power System**" submitted by A. H. M. Sayem, Roll No. 0409062114P, Session: April, 2009, has been accepted as satisfactory in partial fulfillment of the requirement for the degree of **Master of Science in Electrical and Electronic Engineering** on November 17, 2012.

BOARD OF EXAMINERS

1. _____
   Dr. Abdul Hasib Chowdhury — Chairman (Supervisor)
   Associate Professor
   Department of Electrical and Electronic Engineering
   BUET, Dhaka-1000, Bangladesh

2. _____
   Dr. Pran Kanai Saha — Member (Ex-officio)
   Professor and Head
   Department of Electrical and Electronic Engineering
   BUET, Dhaka-1000, Bangladesh

3. _____
   Dr. Md. Quamrul Ahsan — Member
   Professor
   Department of Electrical and Electronic Engineering
   BUET, Dhaka-1000, Bangladesh

4. _____
   Dr. Kazi Mujibur Rahman — Member
   Professor
   Department of Electrical and Electronic Engineering
   BUET, Dhaka-1000, Bangladesh

5. _____
   Dr. Md. Fayyaz Khan — Member (External)
   Professor
   Department of Electrical and Electronic Engineering
   United International University
   Dhaka, Bangladesh

Declaration

It is hereby declared that this thesis titled "**Active Disturbance Rejection Control for Load Frequency Control of Bangladesh Power System**" or any part of it has not been submitted elsewhere for the award of any degree or diploma.

Signature of the Candidate

_____

A. H. M. Sayem

To

my beloved parents Md. Fazlul Haque and Anwara Begum

and

my wife Dr. Seemin Ahmed

Acknowledgements

During the research period in Bangladesh University of Engineering and Technology, I received a great deal of selfless help from a lot of people.

First of all, I would like to thank my advisor, Dr. Abdul Hasib Chowdhury, for his direction, guidance and support. His enthusiasm and inspiration lightened the road of completing this work. I would also like to thank all the committee members for their suggestion and guidance.

I would like to thank my colleague Mohammad Umar Saad for creating the friendly, pleasant working atmosphere and the patient help regarding the simulation of ADRC. Special thanks go to my parents-in-law Naseem Ahmed and Gulshan Akhter for helping me go through all the hardest times.

Lastly, and most importantly, I give my sincere appreciation to my parents Md. Fazlul Haque and Anwara Begum for their unconditional support and making me a better person. My deepest gratitude goes to my beloved wife for her constant love and encouragement.

Abstract

Energy shortage is considered as the most critical infrastructure constraint to the economic growth of Bangladesh. One of the main causes of the supply shortage, among others, is the poor operational efficiency of power plants. For the operation of a large power system maintaining the proper power quality has always been a difficult task. Increasing number of major power grid blackouts that have been experienced around the world including Bangladesh (2007, November and December) in recent years show that today's power system operation requires more careful consideration of all forms of system instability and control problems and introduction of more effective and robust control strategies. In this thesis an Active disturbance rejection control (ADRC) based decentralized Load Frequency Control (LFC) system for Bangladesh Power System (BPS) is developed and a proposal has been made for feedback connections from various load rich areas to generation rich areas to minimize the area control error. The frequency control system maintains frequency and tie-line power flows to specified values in the presence of physical constraints and model uncertainties. As power load demand varies randomly in an interconnected power system, both area frequency and tie-line power interchange also vary. The objectives of LFC are to minimize the transient deviations in these variables (area frequency and tie-line power interchange) and to ensure their steady state errors to be zeros. Unexpected external disturbances, parameter uncertainties and model uncertainties are big challenges for LFC design. As an increasingly popular practical control technique, ADRC has the advantages of requiring little information from the plant model and being robust against disturbances and uncertainties. A solution to the LFC problem based on ADRC is an alternative one. Performance analysis of ADRC is done by comparing with Proportional Integral Derivative (PID) controller and for two area non-reheat and reheat turbine unit. ADRC is also implemented on a large power station. Finally, the design of BPS is done considering its radial connection and proposal is made about feedback connection based on the performance of ADRC. The dynamic model of the power system and the controller design based on the model are elaborated. Simulation results show that ADRC controller is attractive for the LFC problem in terms of its stability and robustness.

Table of Contents

List of Figures

List of Tables

List of Abbreviations

AC	Alternating Current
ACE	Area Control Error
ADRC	Active Disturbance Rejection Control
BPS	Bangladesh Power System
ESO	Extended State Observer
GenCo	Generating Company
GA	Genetic Algorithm
GALMI	Genetic Algorithm and Linear Matrix Inequalities
LFC	Load Frequency Control
MEMS	Micro Electromechanical System
PI	Proportional-Integral
PID	Proportional-Integral-Derivative
TF	Transfer Function

List of Symbols

ΔP_m	Mechanical power
ΔP_v	Valve/gate position change
ΔP_{el}	Electrical power
ΔP_L	Load disturbance
ΔP_{tie}	Tie-line power error
ΔP_e	Input of the equivalent unit in the governor
$\Delta \omega_r$	Rotor speed deviation
$\Delta f / \Delta F$	Frequency error/ generator output
T_{ch}	Time delay
T_{rh}	Low pressure reheat time
F_{hp}	High pressure stage rating
T_g	Time constant of the governor
T_{ij}	Tie-line synchronizing torque coefficient between area i and j
M	Inertia constant of the generator
D	Load damping constant
R	Speed regulation characteristic
B	Frequency response characteristic
U	Controller input
Y	ACE output
L	ESO gain vector
ω_c	Bandwidth of the controller
ω_O	Bandwidth of the observer
b	High frequency gain
G_{NR}	Transfer function of the non-reheat turbine
G_R	Transfer function of the reheat turbine
G_{EU}	Transfer function of the equivalent unit
G_{Tur}	Transfer function of the turbine
G_{Gen}	Transfer function of the generator
G_{PN}	Transfer function of the non-reheat unit
G_{PR}	Transfer function of the reheat unit

Chapter I

Introduction

1.0 Introduction

Satisfactory operation of a power system requires both the active power balance and the reactive power balance between generation and load. Those two balances correspond to two equilibrium points: frequency and voltage. When either of the two balances is broken and reset at a new level, the equilibrium points will float [1]. A good quality of the electric power system requires both the frequency and voltage to remain at standard values during operation. Since loads change randomly and momentarily, it is not possible to maintain both the balances without control. Thus a control system is essential to cancel the effects of load changes and to keep the frequency and voltage at the standard values. The system frequency is highly dependent on the active power while the voltage is highly dependent on the reactive power. Thus the control issue in power systems can be decoupled into two independent problems: one is about the active power and frequency control while the other is about the reactive power and voltage control. The active power and frequency control is referred to as load frequency control (LFC) [1].

Frequency control is becoming more significant today due to the increasing size, the changing structure and the complexity of interconnected power systems. Increasing economic pressures for power system efficiency and reliability requires maintaining system frequency and tie-line flows closer to scheduled values as much as possible. Therefore, in a modern power system, LFC plays an important role, as an ancillary service, in supporting power exchanges and providing better conditions for the electricity trading.

1.1 Background and Present State of the Problem

Increasing number of major power grid blackouts that have been experienced around the world in recent years [2-5], for example, Brazil (1999), Iran (2001, 2002), Northeast USA-Canada (2003), Southern Sweden and Eastern Denmark (2003), Italy (2003), Russia (2005), Bangladesh (2007, November and December) shows that today's power system operations require more careful consideration of all forms of system instability and control problems and to introduce more effective and robust control strategies.

Significant frequency deviations of interconnected system can cause under/over-frequency relaying and disconnect some loads and generations. Under unfavorable conditions, this may result in a cascading failure and system collapse [4]. In the last two decades, many studies have focused on damping control and voltage stability and related issues. However, there has been much less work on power system frequency control analysis and synthesis, while violation of frequency control requirements was known as a main reason for numerous power grid blackouts [2]. Most published research in this area neglects new uncertainties and practical constraints in the liberalized electricity markets and coupling between performance objectives and market dynamics to obtain a good tradeoff between efficiency and robustness [6-7], and furthermore, suggest complex control structures with which may have some difficulties while implementing in real-time applications [8-9]. The establishment of numerous generators units and renewable energy sources in distribution areas and the growing number of independent players is likely to have an impact on the operation and control of the power system, which is already designed to operate with large, central generating facilities.

In summary, the LFC has two major assignments, which are to maintain the standard value of frequency and to keep the tie-line power exchange under schedule in the presences of any load changes [1]. In addition, the LFC has to be robust against unknown external disturbances and system model and parameter uncertainties. The high-order interconnected power system could also increase the complexity of the controller design of the LFC.

In industry, proportional-integral (PI) controllers have been broadly used for decades as the load frequency controllers. A PI controller design on a three-area interconnected power plant is presented in [10], where the controller parameters of the PI controller are tuned using trial-and-error approach.

The LFC design based on an entire power system model is considered as centralized method. In [11] and [12], this centralized method is introduced with a simplified multiple-area power plant in order to implement such optimization techniques on the entire model. However, the simplification is based on the assumption that all the subsystems of the entire power system are identical while they are not. The assumption makes the simulation model in the paper quite different from the real system. Another problem for the centralized methods is that even if the method works well on a low-order test system, it would face an exponentially increasing computation problem with the increase of the system size.

Since the tie-line interfaces give rise to weakly coupled terms between areas, the large-scale power system can be decentralized into small subsystems through treating tie-line signals as disturbances. Numerous control techniques have been applied to the decentralized power systems. In [13–17], decentralized PI or proportional-integral-derivative (PID) controller is reported. Since H_2/H_∞ control is well known for its robustness against parameter uncertainties, the controller has been utilized to solve the decentralized LFC problems in [18-21]. There are also several other modern control theories that have been decentralized solutions of the LFC problem, such as disturbance accommodation control, optimal tracking approach, predictive control scheme and ramp following control, which can be found in [22-25] respectively.

Fuzzy logic control is a method based on fuzzy set theory, in which the fuzzy logic variables can be any value between 0 and 1 instead of just true and false. When the variables are selected, the decision will be made through specific fuzzy logic functions. Research results obtained from applying the fuzzy logic control technique to the decentralized LFC problem have been proposed in [26-29]. Specifically, a fuzzy logic controller developed directly from a fuzzy model of the power system is reported in [26]. A fuzzy logic based tie-line bias control scheme on a two-area multiple-unit power system is introduced in [27] while a similar method on a combined cycle power plant including the comparison between the fuzzy logic control and conventional PID control techniques are reported in [28]. A fuzzy-gain-scheduled PI controller and its implementation on an Iraqi National Super Grid power system can be found in [29]. A comparison between the fuzzy-gain-scheduled PI controller and the traditional PI controller was also included in [29].

Genetic algorithm (GA) is one of the most popular computer intelligence algorithms. It has been verified to be effective to solve complex optimization problem [30] where PI-type controllers tuned via GA and linear matrix inequalities (GALMI) is presented on a decentralized three-area nine-unit power system. In [30], it is found that the structure of the GALMI tuned PI controller is much simpler than that of the H_2/H_∞ controller although the performances of the two methods are equivalent.

Most of the reported solutions of the LFC problem have been tested for their robustness against large step load change. However, very few of the published researches deal with parameter uncertainties. In [31], the authors set up a 15% floating rate for the parameters in one area and successfully controlled the system with an optimally tuned

PID controller. Nevertheless, in [31], a lot of approximations and simplifications have been made during the modeling process of the power systems, on which the controller is designed. The simplified system model has deviated far from the real system. A control technique with a notable robustness against not only parameter uncertainties but also model uncertainties and external load change will be preferred by the power industry.

Active disturbance rejection control (ADRC), an increasingly popular practical control technique, was first proposed by J. Han in [32] and has been modified by Z. Gao in [33, 34]. The design of ADRC only relies on the most direct characteristics of a physical plant, which are input and output. Specifically, the information required for the control purpose is analyzed and extracted from the input and output of the system. ADRC generalizes the discrepancy between the mathematical model and the real system as a disturbance, and rejects the disturbance actively, hence the name active disturbance rejection control. Since ADRC is independent of the precise model information of the physical system, it is very robust against parameter uncertainties and external disturbances [35].

As discussed in [33], ADRC can be understood as a combination of an extended state observer (ESO) and a state feedback controller, where the ESO is utilized to observe the generalized disturbance, which is also taken as an augmented/extended state, and the state feedback controller is used to regulate the tracking error between the real output and a reference signal for the physical plant. In addition, a concept of bandwidth parameterization is proposed in [33] to minimize the number of tuning parameters of ADRC. Using this concept, ADRC only has two tuning parameters, of which one is for the controller, and the other is for the observer. The two tuning parameters directly reflect the response speeds of the ESO and the closed-loop control system respectively. The few tuning parameters also make the implementation of ADRC feasible in practice. The detailed explanations about how to select the tuning parameters for ADRC are provided in [34].

At the beginning of the research of ADRC, time-domain analyses of the controller dominated the publications about it. Recently, a transfer function representation of ADRC was initially presented in [35], where frequency-domain analyses have been successfully conducted on a second-order linear plant.

The closed-loop system with ADRC can be represented by a unity feedback loop with a pre-filter. In the performance analyses in [35], the Bode diagram and the stability margins of

the closed-loop system have been obtained. The unchanged values of the margins against the variations of system parameters demonstrate the notable robustness of ADRC against parameter uncertainties in the plant. Besides [35], a high order ADRC design was developed on a general transfer function form with zeros [36]. The design method was verified on a 3rd order plant with one zero and a known time delay. However, this design approach did not consider the positive zeros for the transfer function form of an inherently unstable system. The physical system with positive zeros is still an unsolved problem for ADRC.

In the past few years, ADRC has been broadly employed in industry. The implementation of ADRC in motion control has been reported in [34]. ADRC is also employed in DC converters, chemical processes, and web tension control as presented in [37-39]. An application of ADRC solution to the control problem of a micro electro-mechanical system (MEMS) gyroscope is presented in [40]. The hardware implementations of ADRC for the MEMS gyroscope were introduced in [41, 42].

Those successful examples reported in the literature [33-42] have validated the effectiveness of ADRC and its great advantages over conventional control techniques such as PID control. ADRC is expected to be applied to more practical control problems in various fields including power systems.

In [43 and 44] Y. Zhang et. el. proposed an ADRC based decentralized load frequency controller for interconnected power systems. A three-area test power system is utilized to test the stability and robustness of ADRC controlled system in the presences of load changes, system parameter variations and tripping of generators. Simulations in time-domain verified the effectiveness of ADRC through successfully regulating the area control error, frequency errors and tie-line power errors.

1.2 Thesis Objective

The objective of the work is to develop a decentralized load frequency controller based on ADRC for Bangladesh Power System (BPS). ADRC is chosen to solve the LFC problem of the BPS because of its robustness against system uncertainties, its simple structure (with only two tuning parameters), and its effective tracking performance.

1.3 Organization of the Thesis

The thesis is organized as follows.

Chapter I is the introductory chapter that represents a brief literature survey on the LFC problem.

Chapter II presents the model of the power generating system. The major components of the power system are discussed in this chapter. A Laplace transform representation of the decentralized area of the power system is also developed in Chapter II.

Chapter III introduces the design strategy of ADRC on an interconnected power system. First the application of ADRC to a second-order motion system is developed. Then ADRC is generalized to an n^{th} order plant with zeros in the transfer function representation of the plant. Finally the development of ADRC on the power system is presented in the chapter.

Chapter IV shows the simulation results of different types of disturbances on three test power systems under the control of ADRC. The first test system is used to compare the control performances between the PID controller and ADRC. The second test system is used to test the robustness of ADRC. The third test system is based on a large power station to verify the effectiveness of ADRC in practical case.

Chapter V presents the simulation results of BPS and suggests a better feedback connection from various generation rich areas to load rich areas considering the same load change.

Chapter VI is the concluding chapter.

Chapter II

Dynamics of the Power Generating System

2.0 Introduction

A comprehensive introduction to the dynamic models of general power systems can be found in [1]. In this chapter, the modeling of a typical power generating system, including the modeling of two types of generating units, the tie-line modeling and the modeling of parallel operation of interconnected areas are introduced.

2.1 Power Generating Units

2.1.1 Turbines

A turbine unit in power systems is used to transform the natural energy, such as the energy from steam or water, into mechanical power (ΔP_m) that is supplied to the generator. In LFC model, there are three kinds of commonly used turbines: non-reheat, reheat and hydraulic turbines, all of which can be modeled by transfer functions. [1]

Non-reheat turbines are first-order units. A time delay (denoted by T_{ch}) occurs between switching the valve and producing the turbine torque. The transfer function can be of the non-reheat turbine is represented as

$$G_{NR}(s) = \frac{\Delta P_m(s)}{\Delta P_v(s)} = \frac{1}{T_{ch}s + 1} \tag{1}$$

where ΔP_v is the valve/gate position change and the load reference set point can be used to adjust the valve/gate positions .

Reheat turbines are modeled as second-order units, since they have different stages due to high and low steam pressure. The transfer function can be represented as

$$G_R(s) = \frac{\Delta P_m(s)}{\Delta P_v(s)} = \frac{F_{hp}T_{rh}s + 1}{(T_{ch}s + 1)(T_{rh}s + 1)} \tag{2}$$

where T_{rh} stands for the low pressure reheat time and F_{hp} represents the high pressure stage rating [31].

2.1.2 Generators

A generator unit in power systems converts the mechanical power received from the turbine into electrical power. But for LFC, we focus on the rotor speed output (frequency of the power systems) of the generator instead of the energy transformation. Since electrical power is hard to store in large amounts, the balance has to be maintained between the generated power and the load demand.

Once a load change occurs, the mechanical power sent from the turbine will no longer match the electrical power generated by the generator. This error between the mechanical (ΔP_m) and electrical powers (ΔP_{el}) is integrated into the rotor speed deviation ($\Delta\omega_r$), which can be turned into the frequency bias (Δf) by multiplying by 2π. The relationship between ΔP_m and Δf is shown in Figure 2.1, where M is the inertia constant of the generator.

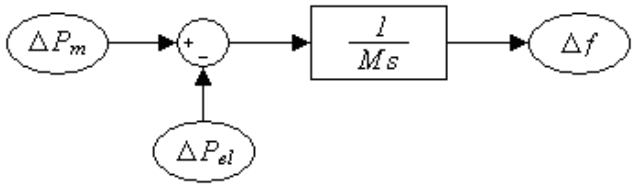

Figure 2.1: Block diagram of the generator

The power loads can be decomposed into resistive loads (ΔP_L), which remain constant when the rotor speed is changing, and motor loads that change with load speed. If the mechanical power remains unchanged, the motor loads will compensate the load change at a rotor speed that is different from a scheduled value, which is shown in Figure 2.2, where D is the load damping constant.

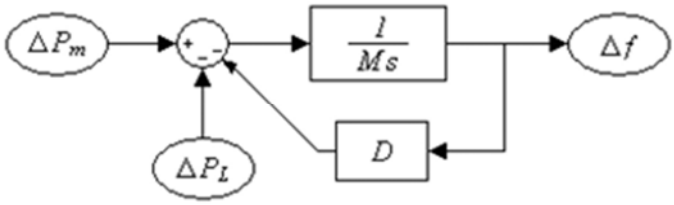

Figure 2.2: Block diagram of the generator with load damping effect

The reduced form of Figure 2.2 is shown in Figure 2.3, which is the generator model that we plan to use for the LFC design. The Laplace-transform representation of the block diagram in Figure 2.3 is

$$\Delta P_m(s) - \Delta P_L(s) = (Ms + D)\Delta F(s) \tag{3}$$

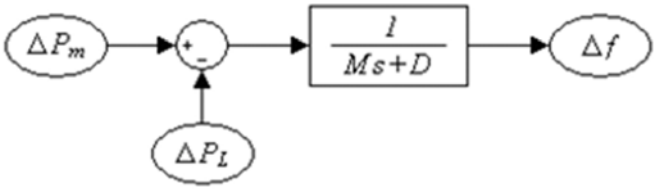

Figure 2.3: Reduced block diagram of the generator with the load damping effect

2.1.3 Governors

Governors are the units that are used in power systems to sense the frequency bias caused by the load change and cancel it by varying the turbine inputs. The schematic diagram of a speed governing unit is shown in Figure 2.4, where R is the speed regulation characteristic and T_g is the time constant of the governor . Without load reference, when the load change occurs, part of the change will be compensated by the valve/gate adjustment while the rest of the change is represented in the form of frequency deviation. The goal of LFC is to regulate frequency deviation in the presence of varying active power load. Thus, the load reference set point can be used to adjust the valve/gate positions so that all the load change is canceled by the power generation rather than resulting in a frequency deviation.

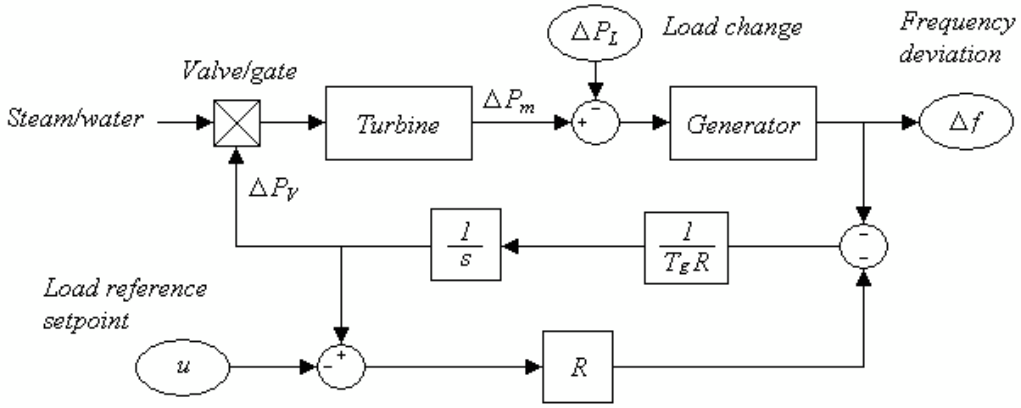

Figure 2.4: Schematic diagram of a modified speed governing unit

The reduced form of Figure 2.4 is shown in Figure 2.5. The Laplace transform representation of the block diagram in Figure 2.5 is given by

$$U(s) - \frac{\Delta F(s)}{R} = (T_g s + 1)\Delta P_v(s) \tag{4}$$

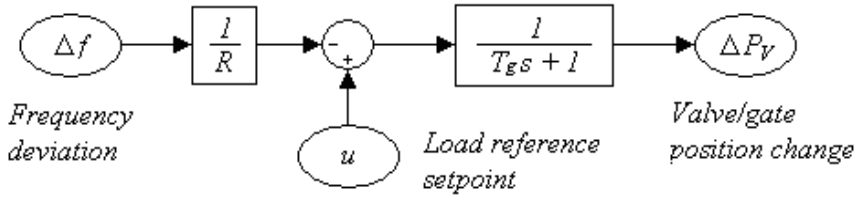

Figure 2.5: Reduced block diagram of the modified speed governing unit

2.2 Interconnected Power Systems

2.2.1 Tie-Lines

In an interconnected power system, different areas are connected with each other via tie-lines. When the frequencies in two areas are different, a power exchange occurs through the tie-line that connects the two areas. The tie-line connections can be modeled as shown in Figure 2.6. The Laplace transform representation of the block diagram in Figure 2.6 is given by

$$\Delta P_{tie}(s) = \frac{1}{s} T_{ij}(\Delta F_i(s) - \Delta F_j(s)) \tag{5}$$

where ΔP_{tie} is the tie-line exchange power between areas i and j, and T_{ij} is the tie-line synchronizing torque coefficient between areas i and j. From Figure 2.6, we can see that the tie-line power error is the integral of the frequency difference between the two areas.

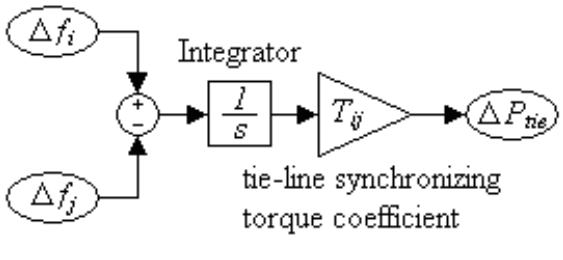

Figure 2.6: Block diagram of the tie-lines

2.2.2 Area Control Error

As discussed in Chapter I, the goals of LFC are not only to cancel frequency error in each area, but also to drive the tie-line power exchange according to the schedule. Since the tie-line power error is the integral of the frequency difference between each pair of areas, if we control frequency error back to zero, any steady state errors in the frequency of the system would result in tie-line power errors. Therefore we need to include the information of the tie-line power deviation into our control input. As a result, an area control error (ACE) is defined as

$$ACE = \sum_{j=1,\ldots,n, j\neq 1} \Delta P_{tie\,ij} + B_i \Delta f_i \tag{6}$$

where B_i is the frequency response characteristic for area i and

$$B_i = D_i + \frac{1}{R_i} \tag{7}$$

This ACE signal is used as the plant output of each power generating area. Driving ACEs in all areas to zeros will result in zeros for all frequency and tie-line power errors in the system.

2.2.3 Parallel Operation

If there is several power generating units operating in parallel in the same area, an equivalent generator will be developed for simplicity. The equivalent generator inertia constant (M_{eq}), load damping constant (D_{eq}) and frequency response characteristic (B_{eq}) can be represented as follows.

$$M_{eq} = \sum_{i=1,....n} M_i \tag{8}$$

$$D_{eq} = \sum_{i=1,....n} D_i \tag{9}$$

$$B_{eq} = \sum_{i=1,....,n} \frac{1}{R_i} + \sum_{i=1,....,n} D_i \tag{10}$$

2.3 Dynamic Model of Single-Area Power Generating Unit

With the power generating units and the tie-line connections of interconnected areas introduced in sections 2.1 and 2.2, a complete form of single-area power generating unit can be constructed as shown in Figure 2.7.

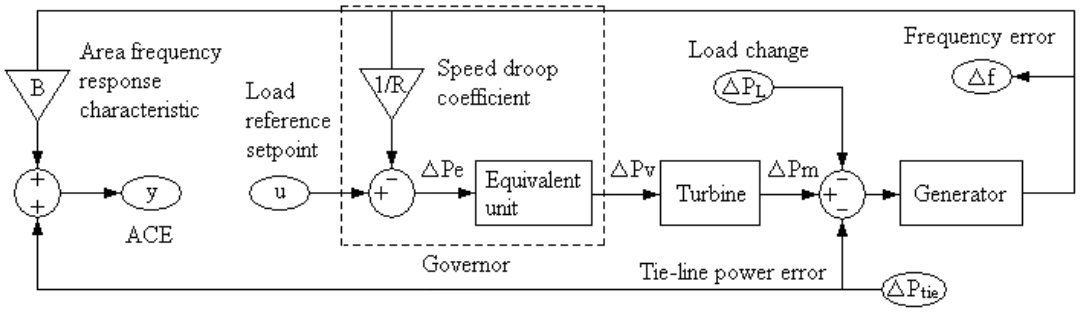

Figure 2.7: Schematic of single-area power generating unit

In Figure 2.7, there are three inputs, which are the controller input *U(s),* load disturbance $\Delta P_L(s)$, and tie-line power error $\Delta P_{tie}(s)$, one ACE output *Y(s)* and one generator output Δf. The term ΔP_e is not in Figure 2.4 because it does not have a physical meaning. We note the input of the equivalent unit in the governor as ΔP_e for simplicity when developing the Laplace transform of the single-area power generating plant.

2.4 The Laplace Transform Model of Single-Area Power Generating Unit

The unit shown in Figure 2.7 is considered. The relationships between the inputs and output in Figure 2.7 can be described as

$$U(s) - \frac{1}{R}\Delta F(s) = \Delta P_e(s) \tag{11}$$

$$G_{EU}(s)\Delta P_e(s) = \Delta P_v(s) \tag{12}$$

$$G_{Tur}(s)\Delta P_v(s) = \Delta P_m(s) \tag{13}$$

$$(\Delta P_m(s) - \Delta P_L(s) - \Delta P_{tie\ ij}(s))G_{Gen}(s) = \Delta F(s) \tag{14}$$

$$Y(s) = B\Delta F(s) + \Delta P_{tie}(s) \tag{15}$$

where $G_{EU}(s)$, $G_{Tur}(s)$ and $G_{Gen}(s)$ are the transfer functions for the equivalent unit, the turbine and the generator respectively.

For the ease of transfer function development, let the transfer function from $\Delta P_e(s)$ that we defined in Figure 2.7 to the mechanical power deviation $\Delta P_m(s)$ be $G_{ET}(s) = Num_{ET}(s)/Den_{ET}(s)$, where $Num_{ET}(s)$ and $Den_{ET}(s)$ are the numerator and denominator of $G_{ET}(s)$ respectively. The representation of $Num_{ET}(s)$ and $Den_{ET}(s)$ may vary from different generating units.

For the non-reheat unit, the combined transfer function of the equivalent unit in governor $G_{ET}(s)$ can be expressed as

$$G_{ET}(s) = \frac{Num_{ET}(s)}{Den_{ET}(s)} = \frac{1}{(T_g s + 1)(T_{ch} s + 1)} \tag{16}$$

For the reheat unit, we have

$$G_{ET}(s) = \frac{Num_{ET}(s)}{Den_{ET}(s)} = \frac{F_{hp} T_{rh} s + 1}{(T_g s + 1)(T_{ch} s + 1)(T_{rh} s + 1)} \tag{17}$$

Define the transfer function of the generator as

$$G_{Gen}(s) = \frac{1}{Den_M(s)} = \frac{1}{Ms + D} \tag{18}$$

where $Den_M(s)$ represents the denominator of $G_{Gen}(s)$. The Laplace transform of the single-area power generating unit can be simplified as

$$Y(s) = G_p(s)U(s) + G_D(s)\Delta P_L(s) + G_{tie}(s)\Delta P_{tie}(s) \tag{19}$$

where

$$G_p(s) = \frac{RBNum_{ET}(s)}{Num_{ET}(s) + RDen_{ET}(s)Den_M(s)} \tag{20}$$

$$G_D(s) = \frac{-RBDen_{ET}(s)}{Num_{ET}(s) + RDen_{ET}(s)Den_M(s)} \tag{21}$$

$$G_{tie}(s) = \frac{Num_{ET}(s) + RDen_{ET}(s)Den_M(s) - RBDen_{ET}(s)}{Num_{ET}(s) + RDen_{ET}(s)Den_M(s)} \tag{22}$$

The modeling of each part in the power generating unit is discussed in this chapter, followed by the Laplace transform development of the decentralized power generating area. The control objective of the LFC problem has been specified as to drive the ACE in each area back to zero. This chapter has laid the groundwork for both the controller design and the constructions of the test power systems.

Chapter III

Design of Active Disturbance Rejection Controller

3.0 Introduction

In the model of the power system developed in Chapter II, the parameter values in the model fluctuate depending on the system and the power flow conditions which change almost every minute. Therefore, dealing with the parameter uncertainties will be an essential factor to choose a control solution to the load frequency control (LFC) problem. After comparing the existing advanced controllers introduced in Chapter I, we selected active disturbance rejection controller (ADRC) for the LFC. In this chapter, the design strategies of ADRC are developed on a general transfer function model of a physical system.

3.1 Active Disturbance Rejection Control

Although we aim to develop ADRC for the high-order power plant, we will introduce the design concept of ADRC on a second order plant for the convenience of explanation.

We consider a motion system that can be described as

$$\ddot{y}(t) + a_1\dot{y}(t) + a_2 y(t) = bu(t) + w(t) \tag{23}$$

where *u(t)* is the input force of the system, *y(t)* is the position output, *w(t)* represents the external disturbance of the system, a_1, a_2 and b are the coefficients of the differential equation. ADRC design approaches can be summarized as four steps.

Step 1: Reformation of the Plant

Equation (23) can be rewritten as

$$\ddot{y}(t) = bu(t) + w(t) - a_1\dot{y}(t) - a_2 y(t) \tag{24}$$

As introduced in [34], the partial information of the plant $-a_1\dot{y}(t) - a_2 y(t)$ can be referred to as internal dynamics. The internal dynamics of the system combined with the external disturbance *w(t)* can form a generalized disturbance, denoted as *d(t)*. Then (24) can be rewritten as

$$\ddot{y}(t) = bu(t) + d(t) \tag{25}$$

The generalized disturbance contains both the unknown external disturbance and the uncertainties in internal dynamics. So, as the generalized disturbance is observed and cancelled by ADRC, the uncertainties included in the disturbance will be canceled as well.

In this way of reforming, all second-order linear systems with different values of a_1 and a_2 can be classified in one category. The systems in this category have two common characteristics: one is the order of the plant, and the other is the high frequency gain b [33]. We will find out that those two characteristics are the essential information required for ADRC design instead of the accurate plant model.

Step 2: Estimation of the Generalized Disturbance

As discussed in Step 1, the generalized disturbance needs to be cancelled after reforming the plant. One way is to obtain the dynamic model of the disturbance and cancel it theoretically. But this idea does not match with the original intention to set up a controller with little information required from the plant. Moreover, the external disturbance could be random and cannot be modeled. Thus another way has to be used to cancel the generalized disturbance rather than to cancel it theoretically. A practical method is to treat the generalized disturbance as an extra state of the system and use an observer to estimate its value. This observer is known as an extended state observer (ESO) [33].

The state space model of (25) is

$$\begin{aligned} \dot{x} &= Ax + Bu + E\dot{d} \\ y &= Cx \end{aligned} \tag{26}$$

In (26), $x = \begin{bmatrix} x_1 \\ x_2 \\ x_3 \end{bmatrix}$,

where $x_1 = y, x_2 = \dot{y}, x_3 = d, A = \begin{bmatrix} 0 & 1 & 0 \\ 0 & 0 & 1 \\ 0 & 0 & 0 \end{bmatrix}$, $B = \begin{bmatrix} 0 \\ b \\ 0 \end{bmatrix}$, $E = \begin{bmatrix} 0 \\ 0 \\ 1 \end{bmatrix}$ $and\ C = [1 \quad 0 \quad 0]$

It is assumed that d has local Lipschitz continuity and $\dot{d}$ is bounded within domain of interests [45]. From (26), the ESO is derived as

$$\dot{z} = Az + Bu + L(y - \hat{y})$$
$$\hat{y} = Cz \tag{27}$$

where $z = [z_1 \quad z_2 \quad z_3]^T$ is the estimated state vector of x and $\hat{y}$ is the estimated system output of y. L is the ESO gain vector and $L = [\beta_1 \quad \beta_2 \quad \beta_3]^T$. To locate all the eigenvalues of the ESO at $-\omega_O$, the values of the elements of the vector L are chosen as

$$\beta_i = \binom{3}{i} . \omega_0^i, i = 1,2,3 \tag{28}$$

with a well tuned ESO, z_i will track x_i closely. Then we will have

$$z_3 \approx x_3 = d \tag{29}$$

From (29), this generalized disturbance *d(t)* can be approximately removed by the time domain estimated value of z_3 .

Step 3: Simplification of the Plant

With the control law

$$u = \frac{u_0 - z_3}{b} \tag{30}$$

the system described in (25) becomes

$$\ddot{y} = b\frac{u_0 - z_3}{b} + d$$

$$\approx (u_0 - d) + d \tag{31}$$

$$\ddot{y} \approx u_0$$

From (31), we can see that with accurate estimation of ESO, the second-order LTI system could be simplified into a pure integral plant approximately. Then a classic state feedback control law could be used to drive the plant output *y* to a desired reference signal.

Step 4: Control Law for the Simplified Plant

The state feedback control law for the simplified plant $\ddot{y} \approx u_0$ is chosen as

$$u_0 = k_1(r - z_1) - k_2 z_2 \tag{32}$$

From (27) z_1 will track y and z_2 will track $\dot{y}$. Then substituting u_0 in $\ddot{y} \approx u_0$ yields

$$\ddot{y} = k_1 r - k_1 y - k_2 \dot{y} \tag{33}$$

The Laplace transform of (33) is

$$s^2 Y(s) + k_2 s Y(s) + k_1 Y(s) = k_1 R(s) \tag{34}$$

The closed-loop transfer function from the reference signal to the position output is

$$G_{cl}(s) = \frac{Y(s)}{R(s)} = \frac{k_1}{s^2 + k_2 s + k_1} \tag{35}$$

Let $k_1 = \omega_c^2 \; and \; k_2 = 2\omega_c$. We will have

$$G_{cl}(s) = \frac{\omega_c^2}{s^2 + 2\omega_c s + \omega_c^2} = \frac{\omega_c^2}{(s + \omega_c)^2} \tag{36}$$

where ω_c represents the bandwidth of the controller. With the increase of the ω_c, the tracking speed of the output of ADRC controlled system will increase as well while the tracking error and overshoot percentage of the output will be decreased. The detail information about the relationship between the parameters ω_c and ω_o and the control performance can be found in [42].

3.2 Generalized ADRC Design of a Plant

In the Laplace domain, a plant with disturbance can be represented as

$$Y(s) = G_p(s).U(s) + W(s) \tag{37}$$

where *U(s)* and *Y(s)* are the input and output respectively, *W(s)* is the generalized disturbance. In (37), the general transfer function of a physical plant $G_p(s)$ can be represented as

$$\frac{Y(s)}{U(s)} = G_p(s) = \frac{b_m s^m + b_{m-1}s^{m-1} + \cdots + b_1 s + b_0}{a_n s^n + a_{n-1}s^{n-1} + \cdots + a_1 s + a_0}, n \geq m \tag{38}$$

where a_i and b_j ($i = 1, \ldots, n, j = 1, \ldots, m$) are the coefficients of the transfer function.

From (25), we can infer that the basic idea of ADRC design is based on the transfer function of the plant without zeros. Thus in order to implement ADRC for the system represented by (37), we need to develop an equivalent model of (38) so that the transfer function only has poles. The error between the two models can be included into the generalized disturbance term.

In order to develop the non-zero equivalent model of (38), the following polynomial long division is conducted on $1 / G_p(s)$.

$$\begin{aligned} \frac{1}{G_p(s)} &= \frac{a_n s^n + a_{n-1}s^{n-1} + \cdots + a_1 s + a_0}{b_m s^m + b_{m-1}s^{m-1} + \cdots + b_1 s + b_0} \ (n \geq m) \\ &= c_{n-m}s^{n-m} + bc_{n-m-1}s^{n-m-1} + \cdots + c_1 s + c_0 + G_{left}(s) \end{aligned} \tag{39}$$

In (39), c_i ($i = 0, \ldots n - m$) are coefficients of the polynomial division result, and the $G_{left}(s)$ is a remainder, which can be represented by

$$G_{left}(s) = \frac{d_{m-1}s^{m-1} + d_{m-2}s^{m-2} + \cdots + d_1 s + d_0}{b_m s^m + b_{m-1}s^{m-1} + \cdots + b_1 s + b_0} \tag{40}$$

In (40), d_j ($j = 0, \ldots, m-1$) are coefficients of the numerator of the remainder. Substituting (39) into (37), we have

$$[c_{n-m}s^{n-m} + bc_{n-m-1}s^{n-m-1} + \cdots + c_1 s + c_0 + G_{left}(s)]Y(s) = U(s) + W'(s) \tag{41}$$

where $W'(s) = {}^{W(s)}\!/_{G_p}$.

(41) can be rewritten as

$$c_{n-m}s^{n-m}Y(s) = U(s) - [c_{n-m-1}s^{n-m-1} + \cdots + c_1 s + c_0 + G_{left}(s)]Y(s) + W'(s) \tag{42}$$

Finally we have

$$s^{n-m}Y(s) = \frac{1}{c_{n-m}}U(s) + D(s) \tag{43}$$

where

$$D(s) = -\frac{1}{c_{n-m}}[c_{n-m-1}s^{n-m-1} + \cdots + c_1 s + c_0 + G_{left}(s)]Y(s) + \frac{1}{c_{n-m}}W'(s) \tag{44}$$

From (39), it can be seen that

$$c_{n-m} = \frac{a_n}{b_m} \tag{45}$$

However, it is difficult to get the expressions of the other coefficients in (39) and (40). Fortunately from the development process of ADRC, *D(s)* is treated as the generalized disturbance and will be estimated in time domain so that we do not actually need the exact expressions for the c_i and d_j ($i = 0, \ldots, n-m, j = 0, \ldots, m-1$) in (39) and (40).

From (43), it is seen that the two characteristics (relative order between input and output and controller gain) have been extracted from the plant by modifying the Laplace transform. Instead of using the order of the plant *n*, the relative order $n - m$ may be utilized as the order of the controlled system. The high frequency gain (denoted as *b*) is still the

ratio between the coefficients of the highest-order terms of the numerator and the denominator.

After obtaining the equivalent order and the high frequency gain, (43) can be rewritten as

$$s^{n-m}Y(s) = bU(s) + D(s) \tag{46}$$

where . $b = {}^{1}/_{c_{n-m}}$

Now ADRC design approach discussed in Section 3.1 may be extended to $n - m$ dimensions. The state space model of (43) is

$$\begin{gathered} sX(s) = AX(s) + BU(s) + EsD(s) \\ Y(s) = CX(s) \end{gathered} \tag{47}$$

where

$$X(s) = \begin{bmatrix} X_1(s) \\ X_2(s) \\ \vdots \\ X_{n-m}(s) \end{bmatrix}_{(n-m)}, \quad A = \begin{bmatrix} 0 & 1 & 0 & \cdots & 0 \\ 0 & \ddots & 1 & \ddots & \vdots \\ \vdots & \ddots & 0 & \ddots & 0 \\ \vdots & \ddots & \ddots & \ddots & 1 \\ 0 & 0 & \ldots & \ldots & 0 \end{bmatrix}_{(n-m)\times(n-m)}, \quad B = \begin{bmatrix} 0 \\ \vdots \\ 0 \\ b \\ 0 \end{bmatrix},$$

$$E = \begin{bmatrix} 0 \\ \vdots \\ 0 \\ 1 \end{bmatrix}_{(n-m)} \qquad C = [1 \quad 0 \quad \ldots \quad 0]_{(n-m)}$$

In (46), *D(s)* is still required to have local Lipschitz continuity and *sD(s)* is bounded with domain of interests [35]. The ESO of the plant is

$$\begin{gathered} sZ(s) = AZ(s) + BU(s)L\left(Y(s) - \hat{Y}(s)\right) \\ \hat{Y}(s) = CZ(s) \end{gathered} \tag{48}$$

where $Z(s) = [Z_1(s) \quad Z_2(s) \quad Z_{n-m}(s)]^T_{(n-m)}$ and $L = [\beta_1 \quad \beta_2 \quad \beta_{n-m}]^T_{(n-m)}$

In order to locate all the eigenvalues of the ESO to $-\omega_O$, the observer gains are chosen as

$$\beta_i = \binom{n-m}{i} . \omega_0^i, \qquad i = 1, \dots, n-m \tag{49}$$

With a well tuned ESO, $Z_i(s)$ will be able to estimate the value of $X_i(s)$ closely ($i = 1, \dots, n-m$). Then we have

$$Z_{n-m}(s) = \widehat{D}(s) \approx D(s) \tag{50}$$

The control law

$$U(s) = (U_0(s) - Z_{n-m}(s))/b \tag{51}$$

will reduce (46) to a pure integral plant, i.e.,

$$s^{n-m}Y(s) = b.\frac{U_0(s) - Z_{n-m}(s)}{b} + D(s) = U_0(s) - \widehat{D}(s) + D(s) \approx U_0(s) \tag{52}$$

The control law for the pure integral plant is

$$U_0(s) = k_1\big(R(s) - Z_1(s)\big) - k_2 Z_2(s) - \cdots - k_{n-m-1} Z_{n-m-1}(s) \tag{53}$$

To further simplify the tuning process, all the closed-loop poles of the PD controller are set to $-\omega_c$. Then the controller gains in (53) have to be selected as

$$k_i = \binom{n-m-1}{n-m-i} . \omega_c^{n-m-1}, i = 1, \dots, n-m-1 \tag{54}$$

In this chapter, the design process of ADRC has been divided into four steps. First, ADRC was implemented on a second–order system. Then it has been extended to a system with a general-form transfer function of any order. Both time-domain and Laplace-domain representation of ADRC are developed in this chapter.

Chapter IV

Performance Analyses of ADRC

4.0 Introduction

In this chapter, ADRC is applied to three kinds of decentralized power systems, which are constructed to test the effectiveness of the controller. The first test system consists of a generating unit with non-reheat turbine, generator and governor. This test system is used to compare the control performances between the PID controller and the ADRC. The second test system consists of generating units, which include non-reheat and reheat turbines, generators and governors. In order to test the robustness of ADRC, it is assumed that all of the parameters in the non-reheat unit of the system have 20% floating rates from their nominal values. The third test system is based on a large power station. It is composed of five non-reheat units and three reheat units that represent the eight units in three interconnected areas. The stability and robustness of ADRC are tested by changing loads on multiple buses at a time. All the simulations in this work have been completed using MATLAB/Simulink.

4.1 Comparison of the Performance of ADRC and PID

The performance of ADRC is compared with PID controller. The test is done on a non-reheat turbine system considering a load change of 0.2p.u. at 2 seconds for both ADRC and PID.

ADRC and PID controlled single-area power system is shown in Figure 4.1. The parameters of the system are obtained from [1, 2] and listed in Table A-1 [Annexure A]. The ADRC and PID parameters are listed in Table A-2 [Annexure A]. The definitions of the parameters have already been given in Chapter II.

Figure 4.2, 4.3 and 4.4 presents the area control error, frequency deviation and tie-line error from both the controller. The figures show that the performance of ADRC is much better than PID. ADRC demonstrates smaller oscillations and faster responses in the ACE and Δf responses than that of the PID controller. However, the control effort of ADRC shows an

overshoot at the switching edge of the load change. This is due to a slight lag of ESO in response to the external disturbance. Nevertheless the overshoot magnitude of ADRC is reasonable. So it will not affect the implementation of the controller in practice.

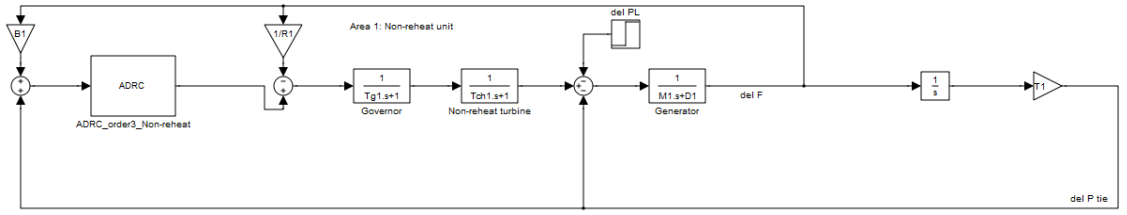

(a)

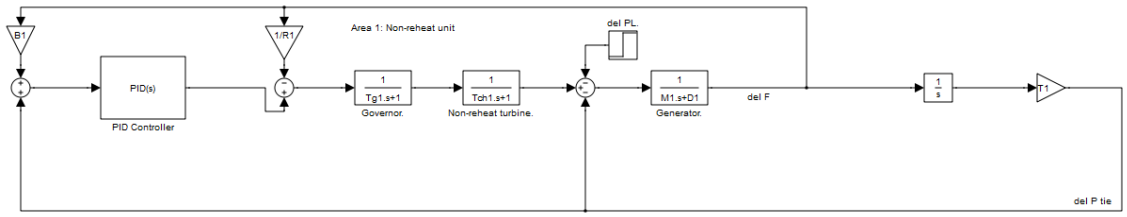

(b)

Figure 4.1: Single-area power system with non-reheat turbine
(a) with ADRC controller (b) with PID Controller

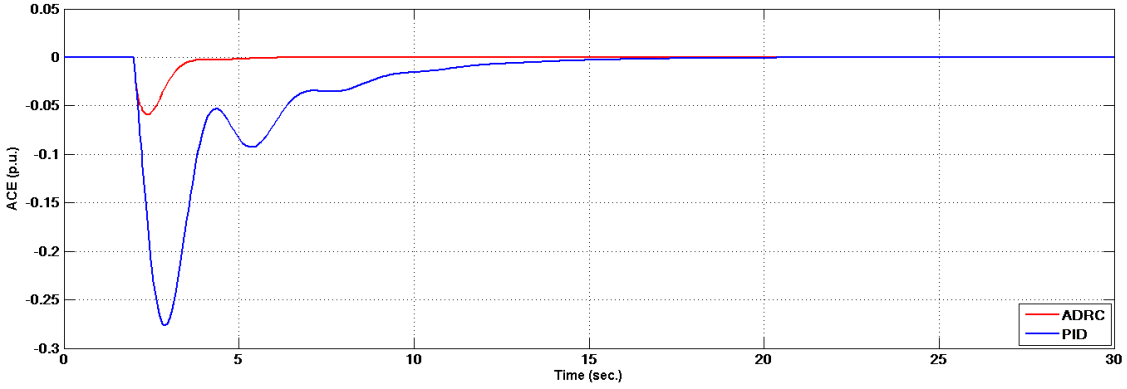

Figure 4.2: Comparison of ACE for ADRC and PID

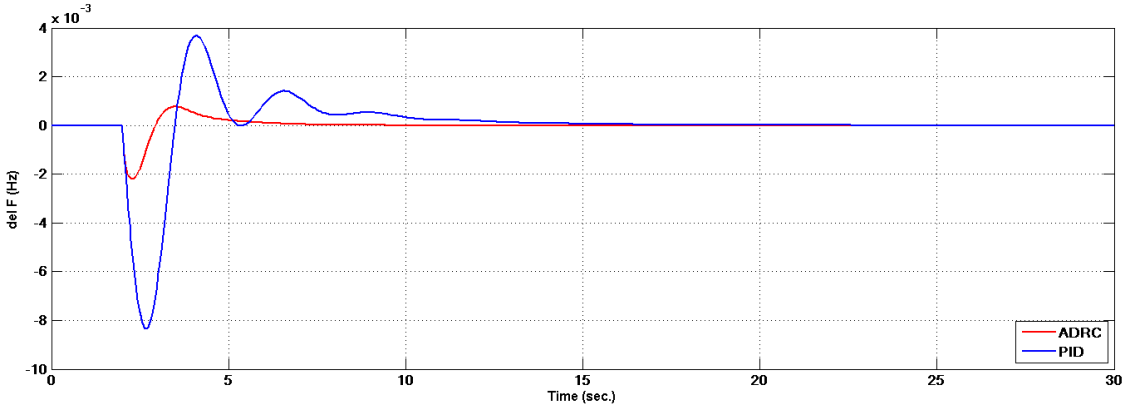

Figure 4.3: Comparison of frequency deviation for ADRC and PID

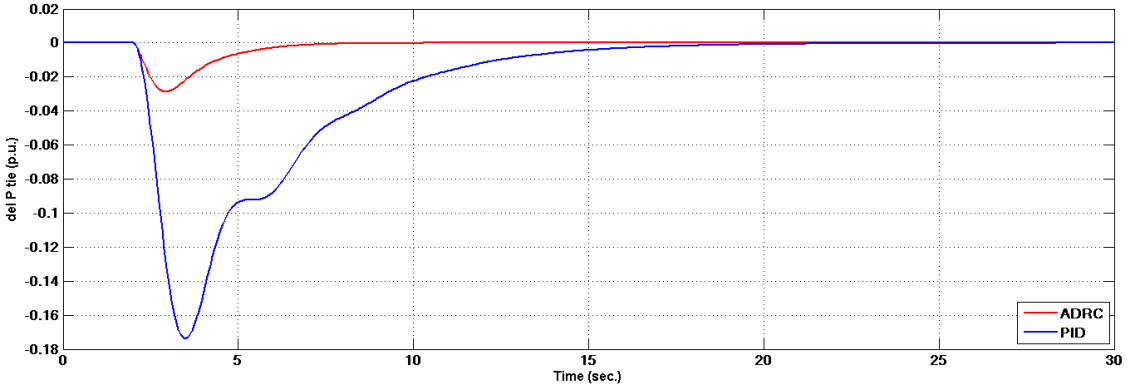

Figure 4.4: Comparison of tie-line error for ADRC and PID

4.2 Application of ADRC on Two-Area Interconnected Power System with Different Generating Units

The second test system consists of two different decentralized areas, which are connected to each other through tie-lines. Each area has three major components, which are turbine, governor and generator. Non-reheat and reheat turbine units are distributed in the two areas respectively. The ADRC controlled interconnected power system is shown in Figure 4.5. The parameters of the system are obtained from [1, 2], and listed in Table A-3 [Annexure A]. The definitions of the parameters have already been given in Chapter II.

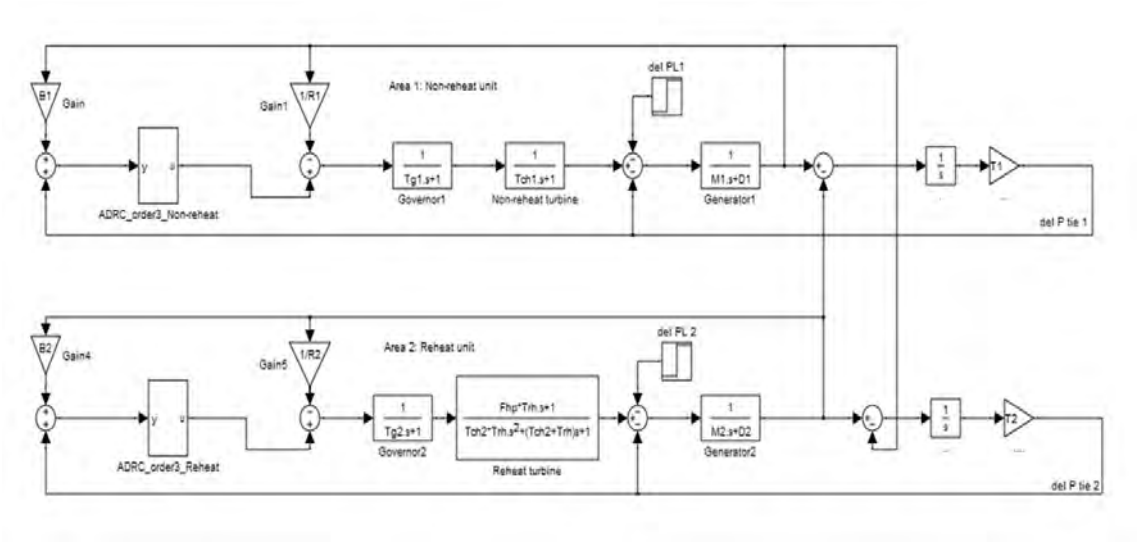

Figure 4.5: ADRC controlled two-area power system with non-reheat and reheat turbines

For each decentralized area in Figure 4.5, an ADRC is designed based on the transfer function $G_P(s)$ in (20). The transfer functions of the non-reheat $(G_{PN}(s))$ and reheat $(G_{PR}(s))$ units are given by (55) and (56) respectively

$$G_{PN}(s) = \frac{1.05}{0.015s^3 + 0.2015s^2 + 0.52s + 1.05} \tag{55}$$

$$G_{PR}(s) = \frac{2.205s + 1.05}{0.21s^4 + 1.801s^3 + 3.928s^2 + 2.975s + 1.05} \tag{56}$$

According to the discussions in Chapter III, ADRC (including its ESO) for area 1 can be designed and represented by the following equations.

$$sZ(s) = (A - LC)Z(s) + BU(s) + LY(s) \tag{57}$$

$$U_0(s) = k_1\big(R(s) - Z_1(s)\big) - k_2Z_2(s) - k_3Z_3(s) \tag{58}$$

$$U(s) = \frac{U_0(s) - Z_4(s)}{b} \tag{59}$$

where, $Z(s) = \begin{bmatrix} Z_1(s) \\ Z_2(s) \\ Z_3(s) \\ Z_4(s) \end{bmatrix}, A = \begin{bmatrix} 0 & 1 & 0 & 0 \\ 0 & 0 & 1 & 0 \\ 0 & 0 & 0 & 1 \\ 0 & 0 & 0 & 0 \end{bmatrix}, B = \begin{bmatrix} 0 \\ 0 \\ b \\ 0 \end{bmatrix}, C = [1 \quad 0 \quad 0 \quad 0], L = \begin{bmatrix} 4\omega_0 \\ 6\omega_0^2 \\ 4\omega_0^3 \\ \omega_0^4 \end{bmatrix},$

$k_1 = \omega_c^3, k_2 = 3\omega_c^2, k_3 = 3\omega_c$

ADRCs for the other area have the similar structure to ADRC for area 1. The design parameters of ADRCs in different areas are given in Table A-4 [Annexure 1].

The performance of ADRC is tested for three cases of system parameters. A 0.1 p.u. step load change is applied to the two different areas at t = 2 and 7 seconds respectively. In the different cases, the parameter values of the non-reheat unit in area 1 will have different values. In the following two cases, the controller parameter values of ADRC remain unchanged.

In case 1, the parameters of the non-reheat unit in area 1 are chosen to have nominal values. The effectiveness of ADRC will be tested in this case by simulating the closed-loop control system in Figure 2.7. In our simulation results, area 1 is denoted as the area with non-reheat unit (or non-reheat) and area 2 is denoted as the area with reheat unit (or reheat). The system responses for two different areas are shown in Figures 4.6, 4.7, and 4.8. Figure 4.6 illustrates the Area Control Error (ACE) outputs of the two different areas, Figure 4.7 illustrates the frequency errors (Δf) of the two different areas and Figure 4.8 shows the tie-line power errors of the two areas. From the simulation results, we can see that the ACEs, the frequency errors and the tie-line power deviations have been driven to zero by ADRC in the presences of load power changes. The average settling time in the system responses is around 3 seconds.

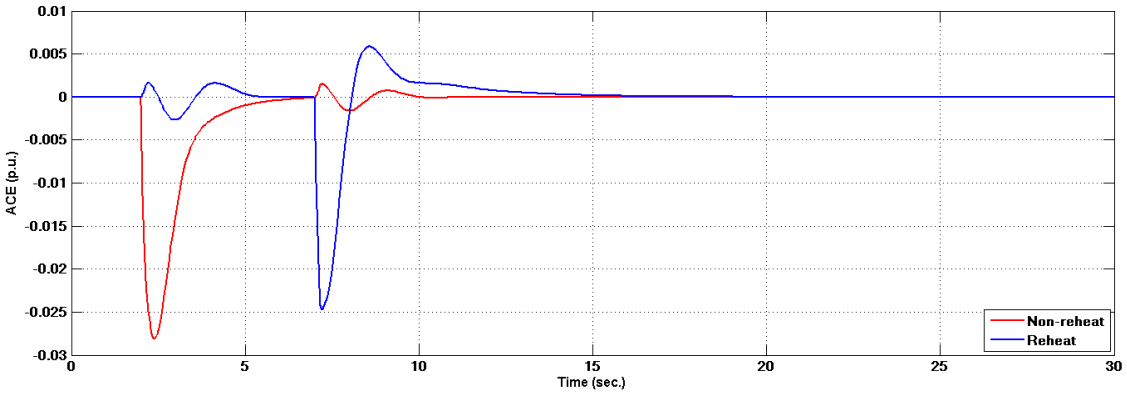

Figure 4.6: ACEs of the two-area power systems

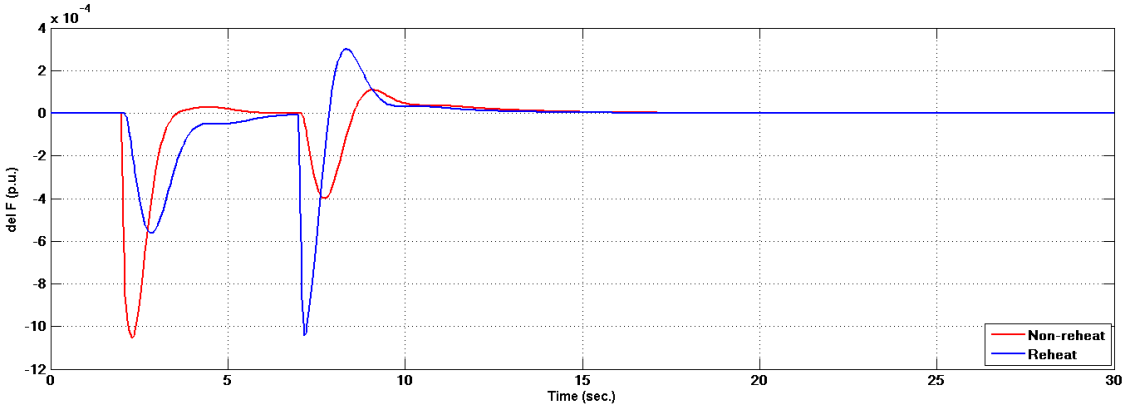

Figure 4.7: Frequency errors of the two-area power systems

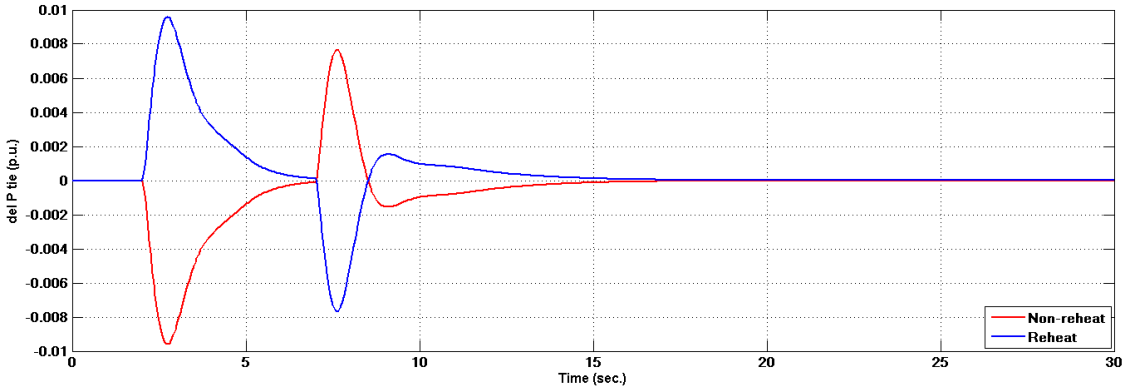

Figure 4.8: Tie-line power errors of the two-area power systems

In case 2, in order to test the robustness of ADRC, the variations of all of the parameters (M_1 , D_1 , T_{ch1} , T_{g1} , R_1 , *and* T_1) of the non-reheat unit in the first area are assumed to be 20% and -20% of their nominal values respectively. However, the controller parameters of ADRC are not changed with the variations of the system parameters. The responses of area 1 are shown in Figures 4.9, 4.10 and 4.11. Figure 4.9 illustrates the ACE outputs of area 1 with the variant parameter values for the non-reheat unit, Figure 4.10 illustrates the frequency errors of area 1 with the variant parameter values for the non-reheat unit and Figure 4.11 shows the tie-line power errors of area 1 with the variant parameter values for the non-reheat unit. From the simulation results, we can see that despite such large parameter variations, the system responses do not show notable differences from the results in Figures 4.9, 4.10 and 4.11. Therefore the simulation results demonstrate the robustness of ADRC against system parameter variations. If we change the system parameters for reheat unit, the same conclusion is obtained since the model for each area is similar to the other.

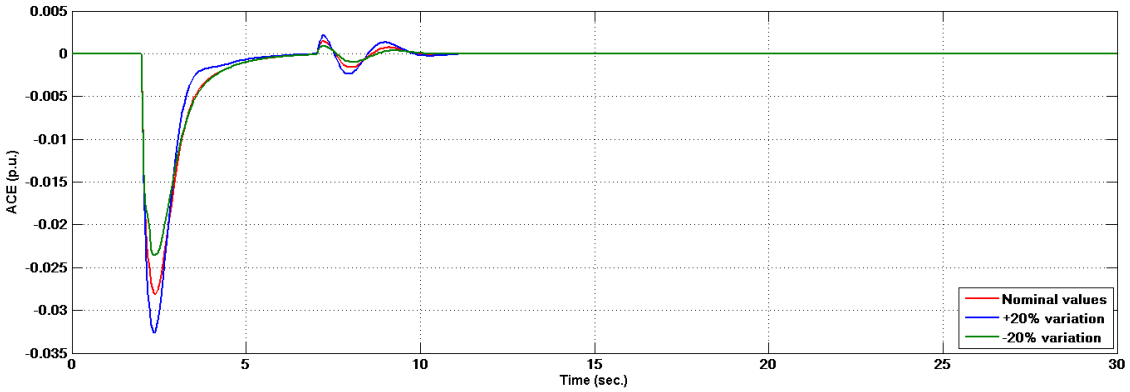

Figure 4.9: ACEs of area 1 with variant parameter values for non-heat unit

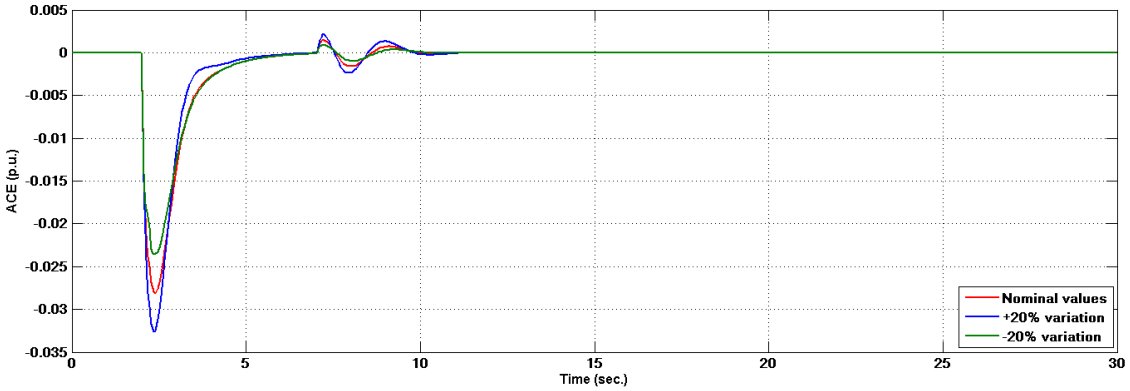

Figure 4.10: Frequency errors of area 1 with variant parameter values for non-reheat unit

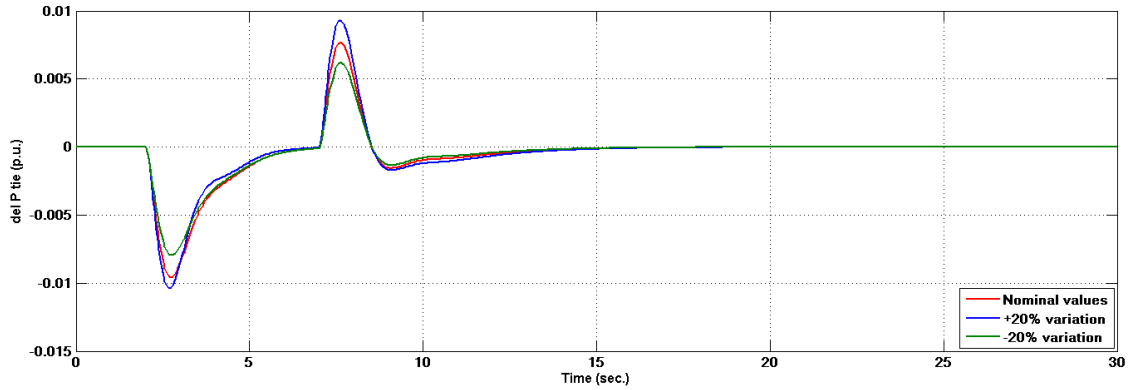

Figure 4.11: Tie-line power errors of area 1 with variant parameter values for non-reheat unit

4.3 Application of ADRC on Large Power Station

Consider a large power station that is equivalent to the second largest power station in Bangladesh. The installed capacity by its 3 areas with 8 units is 724 MW and present de-rated capacity is 642 MW. It fulfills about 15% of power requirements of the country.

The three plants are:

Plant 1: Thermal Power Plant (TPP)

Two steam units of 64 MW- Unit # 1 & 2.

Plant 2: Combined Cycle Power Plant (CCPP)

Gas turbine units-GT1 and GT2 of capacity 56 MW each and one steam turbine (ST) of capacity 34 MW with waste heat recovery Boiler.

Plant 3: Thermal Power Plant (TPP)

Unit # 3, Unit # 4 and Unit # 5 each of 150 MW capacity.

There are 5 non-reheat and 3 reheat turbine units in the large power station. Based on this the whole plant was constructed for simulation. All the units were connected with each other to observe the tie-line error if there is load change in any one unit. The output shows the area control error, frequency deviation and tie line error for these 8 units.

ADRC based controller is implemented on each unit of the system shown in Figure 4.12. In Figure 4.12, it is considered that unit 1 and 2 are under plant 1 which consist two non-reheat type turbines, unit 3, 4 and 5 are under plant 2 which consists three reheat type turbines, unit 6, 7 and 8 are under plant 3 which consists two non-reheat type turbines. The parameters of the system are listed in Table A-5 [Annexure A] and the ADRC parameters are listed in Table A-6 [Annexure A].

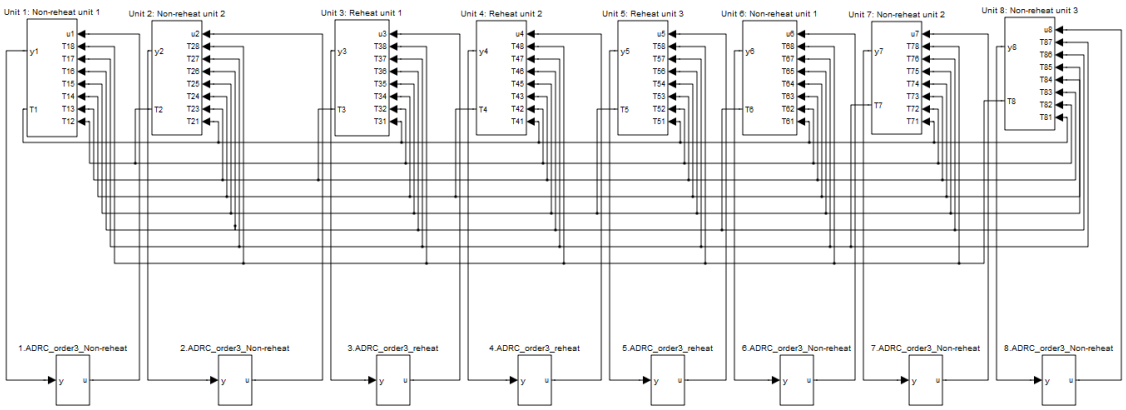

Figure 4.12: Dynamic model of the large power station

Unit 1 of Figure 4.12 named Unit 1: Non-reheat unit 1 is modeled according to Figure 4.13. In this area the main building blocks are governor, non-reheat turbine and generator. ADRC is designed based on the transfer function $G_P(s)$ in (20).

The modeling of all the non-reheat units is similar to unit 1.

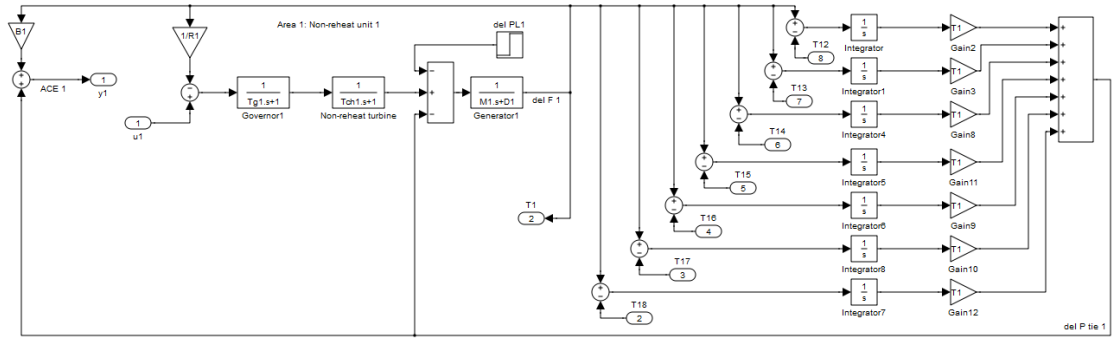

Figure 4.13: Dynamic model of Unit 1: Non-reheat unit 1

Unit 3 of Figure 4.12 named Unit 3: Reheat unit 1 is modeled according to Figure 4.14. In this area the main building blocks are governor, reheat turbine and generator. ADRC is designed based on the transfer function $G_P(s)$ in (20).

The modeling of all the reheat units is similar to unit 3.

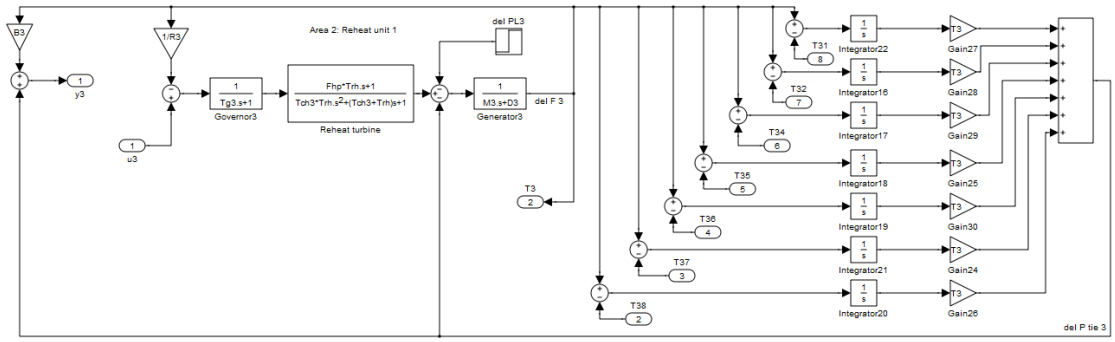

Figure 4.14: Dynamic model of Unit 3: Reheat unit 1

A step load change with large amplitude is added to each unit. The purpose of this case is to test the robustness of the controllers against large disturbances. The amplitudes of the load changes for the eight units are ΔP_{L1} = 0.9 p.u., ΔP_{L2} = 0.8 p.u., $\Delta PL3$ =0.7 p.u., ΔP_{L4} =0.6 p.u., ΔP_{L5} =0.5 p.u., ΔP_{L6} =0.4 p.u., ΔP_{L7} =0.3 p.u. and ΔP_{L8} =0.2 respectively. The power loads are added to the systems at t = 2 seconds. The ACE, Δf and the control effort for ADRC controlled systems are shown in Figures 4.15, 4.16 and 4.17. ADRC demonstrates smaller oscillations and faster responses in the ACE and Δf responses.

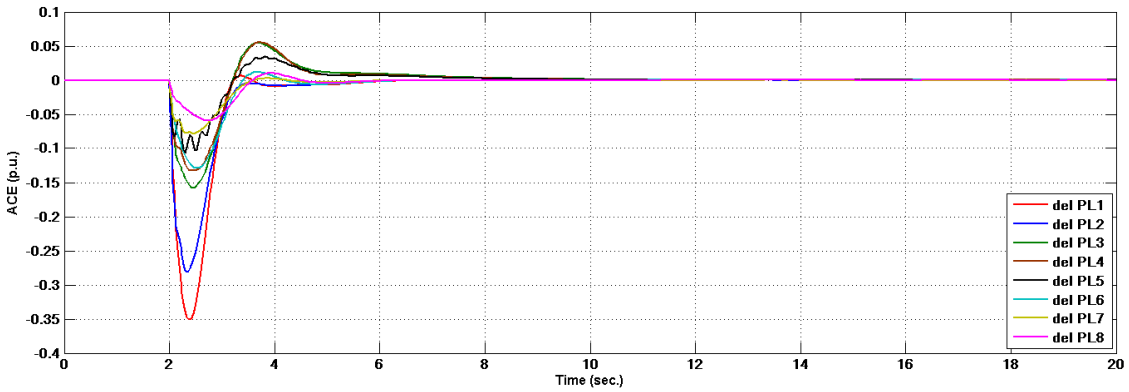

Figure 4.15: ACEs of the large power station for various load changes

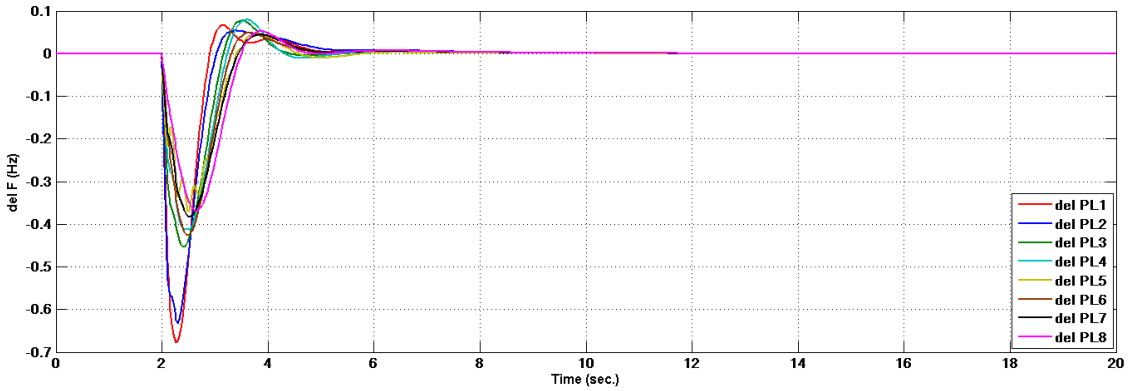

Figure 4.16: Frequency errors of the large power station for various load changes

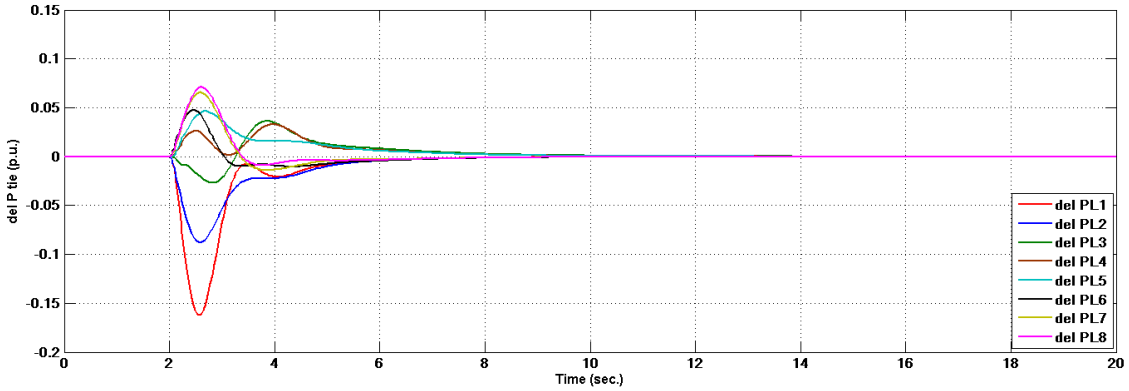

Figure 4.17: Tie-line power errors of the large power station for various load changes

The simulation results in this chapter verified the effectiveness of ADRC on the LFC problem in three aspects. First of all, ADRC is able to cancel the ACE to satisfy the LFC requirements of maintaining the standard frequency and keeping the tie-line power exchange according to the schedule. Secondly, ADRC is effective to cancel both random and large load disturbances. Thirdly, ADRC is able to resist the interferences to the controller design of parameter uncertainties. Thus, ADRC is considered to be a suitable control technique for LFC solution.

Chapter V

Simulation on Bangladesh Power System

5.0. Introduction

Bangladesh Power System (BPS) is a small system with an installed capacity of around 6700 MW and an annual peak demand of around 7000 MW. The transmission system of BPS has formed an integral grid of two voltage levels of 132 and 230 kV. It supplies electricity to the whole country, geographically divided into two regions by the rivers Padma and Jamuna. That is, the transmission system has two major regions connected through two tie line, known as East-West Interconnector -1 and -2.

5.1 Overview of Bangladesh Power System

The BPS grid network is inherently radial in nature. Fig. 5.1 shows the BPS grid in terms of a number of regions. The figure clearly shows that the regions are like islands connected radially to the Dhaka region. The status of different islands in terms of generation capacity and loads of a typical day for 2010 is given in Table 5.1. The table shows that most of the islands are load rich. A load rich island is the one whose available generation is less than the load and generation rich island has available generation more than its load. [46]

Only Dhaka and Sylhet regions are generation rich. In the Dhaka region only three generator buses are considered, namely Ashuganj, Ghorashal and Meghnaghat. These three buses are connected to tie-lines that supply power to the load rich regions. Moreover, the power stations at these locations generate most of the power in the regions and practically contribute towards maintaining the system frequency. In the Sylhet region, the Shahjibazar bus acts both as a generator bus and a tie-bus that supply power to other regions through the Ashuganj.

The Khulna-Barishal regions acts as a net load to the Ishwardi bus in the North Bengal region. Power from Dhaka region flows to this region through Ishwardi bus. As such this region is not modeled as a separate load.

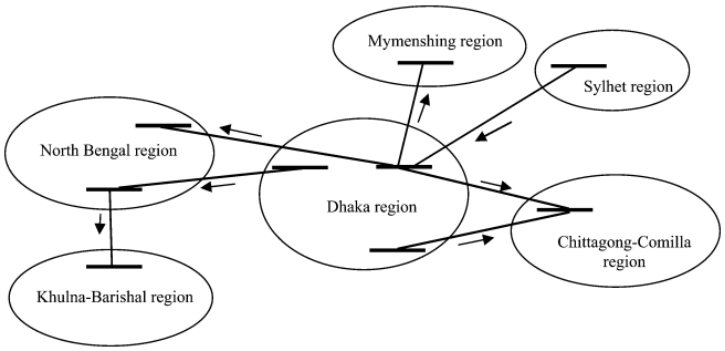

Figure 5.1: Radial nature of Bangladesh Power System

Table 5.1: Status of different radially connected regions of BPS

Description of the island	Available generation (MW)	Demand (MW)	Status of the island
Dhaka region	2390	1450	Generation rich
Ctg., Comilla, Noakhali region	233	698	Load rich
Sylhet region	308	176	Generation rich
Mymenshing region	133	250	Load rich
North Bengal region	421	645	Load rich
Khulna-Barisal region	205	464	Load rich

5.2 Application of ADRC on Bangladesh Power System

ADRC based load frequency controller is constructed to apply in BPS. The BPS is modeled considering only Dhaka and Sylhet regions are generation rich. The load rich regions are modeled as loads at the tie buses in that region and equivalent to the tie flow in that bus in a typical day. The tie buses considered as load bus are at Ishwardi, Sirajganj, Kishoreganj and Comilla (North). The generation rich areas are modeled as power plants at four tie buses, namely Ashuganj, Ghorasal, Meghnaghat and Shahjibazar, the first three being located in the Dhaka region and the last one in the Sylhet region.

It will be considered that the four generation rich areas consist of four generators and four load rich areas consist of four loads. According to the present grid connection of Bangladesh Ashuganj is connected with Ghorashal, Meghnaghat and Shahjibazar, Ghorashal is connected with Ashuganj and Meghnaghat, Meghnaghat is connected with Ghorashal and Ashuganj and Shahjibazar is connected with Ashuganj as Figure 5.2. Each load will be connected to all the

generators (Figure 5.2) to compare the performance of area control error, frequency deviation and tie-line error using ADRC for the same load change from each load area separately. Selecting the minimum value of ACE from a specific load area to each generator, a feedback connection from specific load area to specific generator area will be proposed to minimize the frequency deviation from the reference value.

The effect of load changes on specific generation rich area from various load rich areas will depend on the distance between them because tie-line synchronizing coefficient (T_{ij}) is dependent on the reactance of the transmission line.

$$T = \frac{\omega_{e0}}{X} \tag{60}$$

where X is the reactance.

The exact reactance of various transmission lines of BPS is used in this work. We will have to find an optimum connection considering less settling time and less overshoot for reduced error level and for maintaining rated frequency during load changes. Comparing the performance by changing the same load from a net load area to all four generating stations, the variations from the rated frequency will be computed.

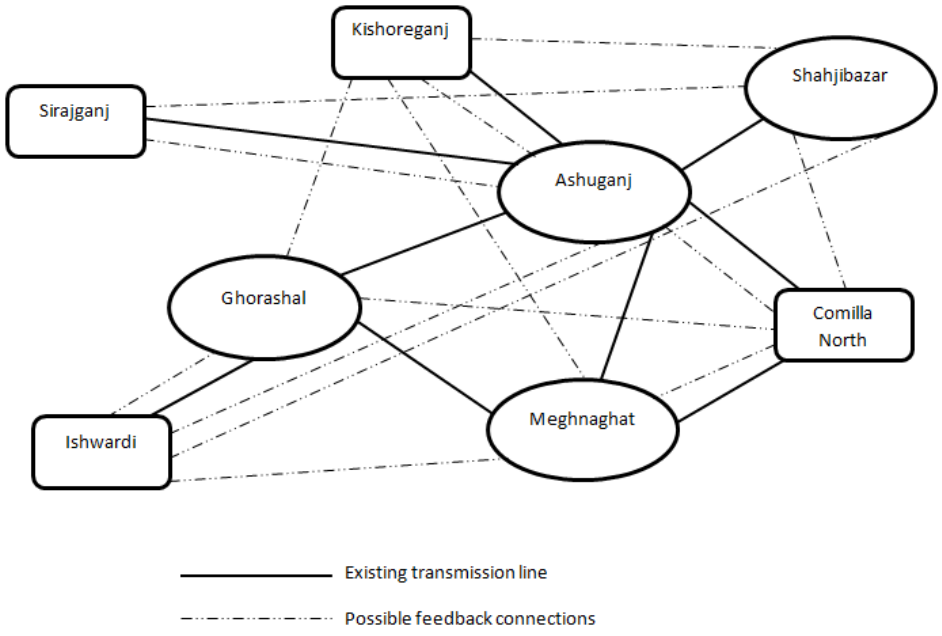

Figure 5.2: Schematic diagram of BPS for simulation with ADRC

The effectiveness of ADRC on the LFC problem of BPS will be verified. If we make feedback connections according to the above discussion then ADRC is able to cancel the ACE to satisfy the LFC requirements of maintaining the standard frequency and keeping the tie-line power exchange according to the schedule. By this way, it will be easy to propose a modified feedback connections from four load rich areas of BPS based on ADRC for better load frequency control performance.

5.2.1 Modeling of BPS with ADRC

ADRC based controller is implemented on each area of the system in Figure 5.3. For simplicity the whole BPS is divided into four areas. The four subsystem blocks named Ashuganj Power Plant, Ghorashal Power Plant, Meghnaghat Power Plant and Shajibazar Power plant represent the four power plants. Each power plant block has four load disturbance signals as input. These signals signify any load change from the system balanced condition at the four load buses and fed to the power plant blocks through feedback connection. The load change signal may be calculated at the load buses by measuring the line power flows except the flow at those buses and transmitted to the power plants over optical communication network.

The input and output of each power plant block are mentioned in Table 5.2.

Table 5.2: Input and Output of each power plant block

Block Name	Input as load change from	Output
Ashuganj Power Plant	Sirajganj (del PL_Si to A) Kishoreganj (del PL_Ki to A) Comilla North (del PL_Cn to A) Ishwardi (del PL_Is to A)	Frequency deviation (del F_A) Area Control Error (ACE_A) Tie-line flow deviation (del P tie_A)
Ghorashal Power Plant	Sirajganj (del PL_Si to G) Kishoreganj (del PL_Ki to G) Comilla North (del PL_Cn to G) Ishwardi (del PL_Is to G)	Frequency deviation (del F_G) Area Control Error (ACE_G) Tie-line flow deviation (del P tie_G)
Meghnaghat Power Plant	Sirajganj (del PL_Si to M) Kishoreganj (del PL_Ki to M) Comilla North (del PL_Cn to M) Ishwardi (del PL_Is to M)	Frequency deviation (del F_M) Area Control Error (ACE_M) Tie-line flow deviation (del P tie_M)
Shahjibazar Power Plant	Sirajganj (del PL_Si to S) Kishoreganj (del PL_Ki to S) Comilla North (del PL_Cn to S) Ishwardi (del PL_Is to S)	Frequency deviation (del F_S) Area Control Error (ACE_S) Tie-line flow deviation (del P tie_S)

The Tie line synchronizing coefficients between Ashuganj to Ghorashal (T_{12}), Ahuganj to Meghnaghat (T_{13}), Ashuganj to Shahjibazar (T_{14}), Ghorashal to Ashuganj (T_{21}), Ghorashal to Meghnaghat (T_{23}), Meghanghat to Ashuganj (T_{31}), Meghnaghat to Ghorashal (T_{32}), and Shahjibazar to Ashuganj (T_{41}) is dependent on the distance between them and the reactance of the corresponding transmission line. Ashuganj, Ghorashal, Meghnaghat and Shahjibazar are connected according to the existing transmission line of BPS. The tie- line synchronizing coefficients between Sirajganj to four generation rich areas (T_{51}, T_{52}, T_{53}, T_{54}), between Kishoreganj to four generation rich areas (T_{61}, T_{62}, T_{63}, T_{64}), between Comilla (North) to various generation areas (T_{71}, T_{72}, T_{73}, T_{74}) and Ishwardi to various generation areas (T_{81}, T_{82}, T_{83}, T_{84}) are also calculated based on equation (60).

The design parameters of the system are listed in Table A-7 [Annexure A] and the ADRC parameters are listed in Table A-8 [Annexure A].

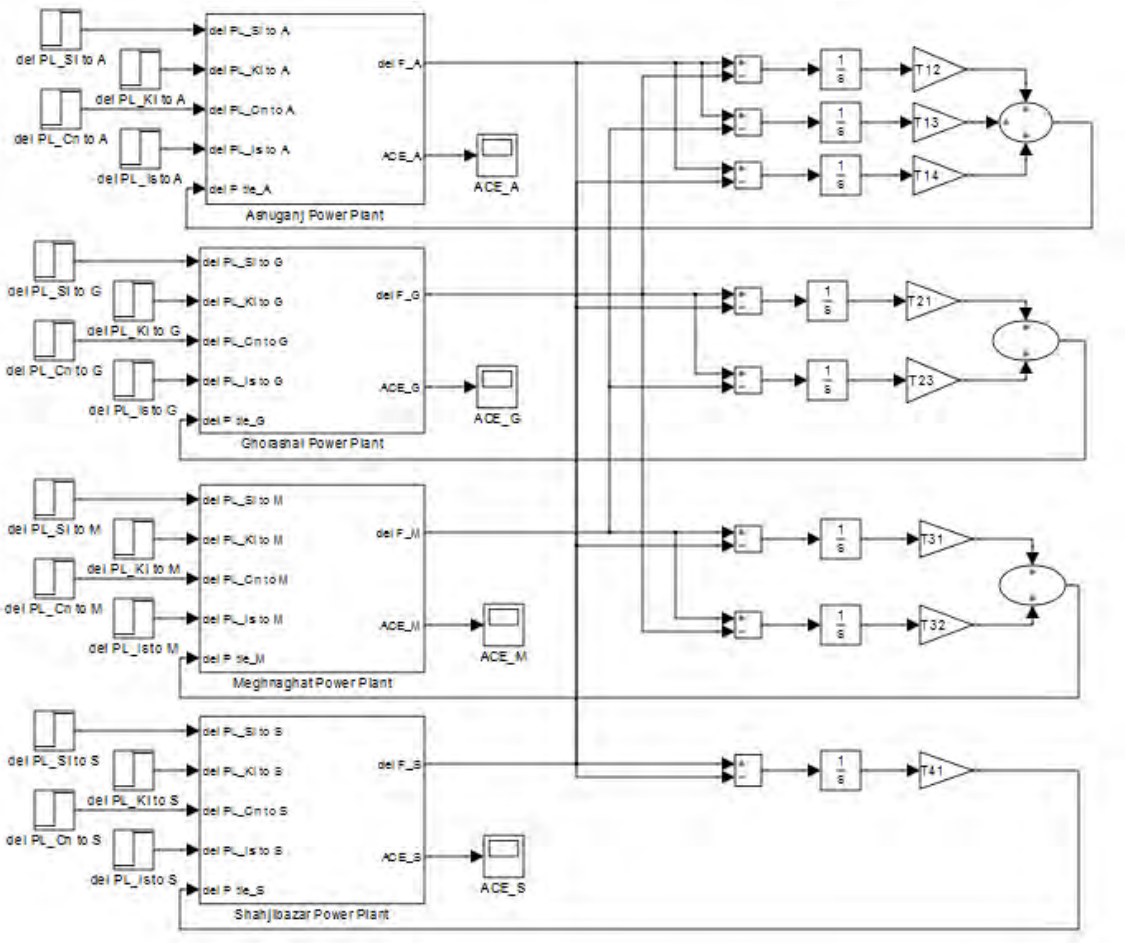

Figure 5.3: Dynamic model of Bangladesh Power System

Area 1 in Figure 5.3 named Ashuganj Power Plant is modeled according to Figure 5.4. In this area the main building blocks are governor, reheat turbine and generator. ADRC is designed based on the transfer function G_P (s) in (20). The transfer functions of the reheat $(G_{PR}(s))$ unit is given by

$$G_{PR}(s) = \frac{2.205s + 1.05}{0.21s^4 + 1.801s^3 + 3.928s^2 + 2.975s + 1.05} \tag{61}$$

According to the discussions in Chapter III, ADRC (including its ESO) for Ashuganj Power Plant can be designed and represented by the following equations.

$$sZ(s) = (A - LC)Z(s) + BU(s) + LY(s) \tag{62}$$

$$U_0(s) = k_1\big(R(s) - Z_1(s)\big) - k_2 Z_2(s) - k_3 Z_3(s) \tag{63}$$

$$U(s) = \frac{U_0(s) - Z_4(s)}{b} \tag{64}$$

where .

$$Z(s) = \begin{bmatrix} Z_1(s) \\ Z_2(s) \\ Z_3(s) \\ Z_4(s) \end{bmatrix}, A = \begin{bmatrix} 0 & 1 & 0 & 0 \\ 0 & 0 & 1 & 0 \\ 0 & 0 & 0 & 1 \\ 0 & 0 & 0 & 0 \end{bmatrix}, B = \begin{bmatrix} 0 \\ 0 \\ b \\ 0 \end{bmatrix}, C = [1 \quad 0 \quad 0 \quad 0], L = \begin{bmatrix} 4\omega_0 \\ 6\omega_0^2 \\ 4\omega_0^3 \\ \omega_0^4 \end{bmatrix},$$

$k_1 = \omega_c^3,$

$k_2 = 3\omega_c^2,$

$k_3 = 3\omega_c$

ADRCs for the other three areas have the similar structure to ADRC for Ashuganj Power Plant.

The modeling of other three areas are similar to Ashuganj Power Plant.

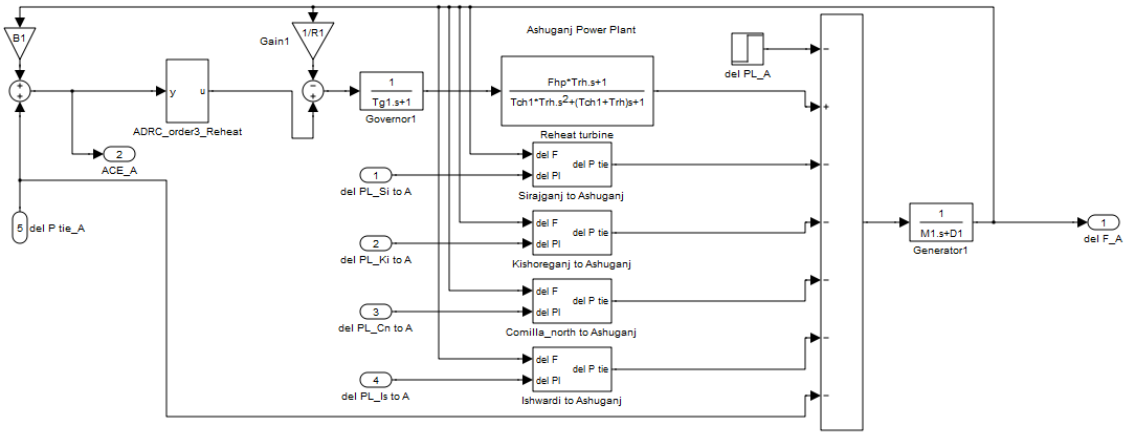

Figure 5.4: Dynamic model of Ashuganj power plant

In Figure 5.4 the block named Sirajganj to Ashuganj corresponds to the load change from Sirajganj to Ashuganj. The detail diagram of this subsystem is given in Figure 5.5. Here a non-reheat turbine is used with governor and generator. A third order ADRC is applied in the block. The output of the generator of this block is frequency deviation which is first integrated then multiplied by tie-line synchronizing coefficients between Sirajganj to Ashuganj (T_{51}) to get the tie-line flow deviation (del P tie).

Other three blocks in Figure 5.4 named Kishoreganj to Ashuganj, Comilla_north to Ashuganj and Ishwardi to Ashuganj are designed similar to Figure 5.5 to calculate the effect of load change to Ashuganj from other three load rich areas.

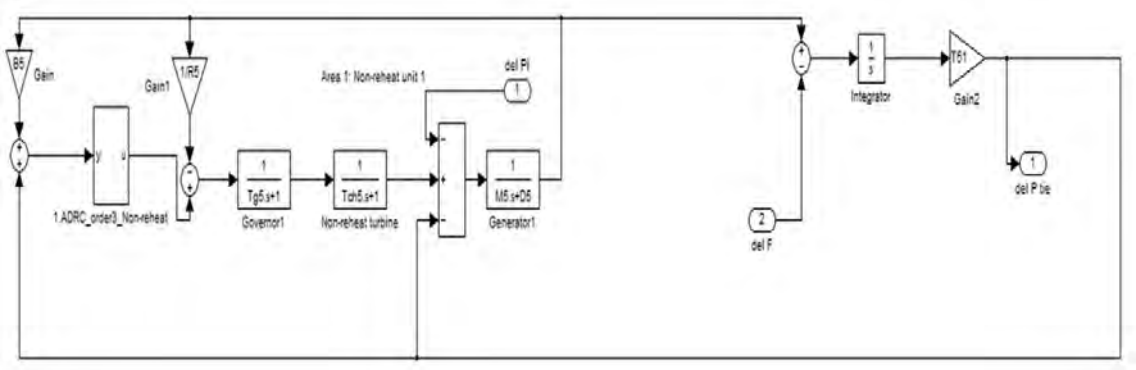

Figure 5.5: Dynamic model of load change from Sirajganj to Ashuganj

Finally, combining all these Figures (5.3 to 5.5), the complete subsystem of Ashuganj Power Plant is ready to calculate the effect of ACE, frequency deviation and tie-line flow deviation if there is any load change in Sirajganj to Ashuganj or Kishoreganj to Ashuganj or Comilla (North) to Ashuganj or Ishwardi to Ashuganj feedback connection.

In the similar way other three blocks named Ghorashal Power Plant, Meghnaghat Power Plant and Shahjibazar Power Plant are constructed to calculate the effects of load change from the four load rich areas.

If the blocks Ashuganj Power Plant, Ghorashal Power Plant, Meghnaghat Power Plant and Shahjibazar Power Plant are combined and connected with each other according to the existing transmission line of BPS using tie-line synchronizing coefficients between any two areas, then the outcome will be the overall power system of Bangladesh. In this way Figure 5.3 represents the dynamic model of BPS.

5.2.2 Simulation of BPS with ADRC

The simulation of BPS is done to propose proper feedback connections from four load rich areas to four generation rich areas. During all simulation the load change is considered 0.1 p.u. in t=2 sec. The whole simulation process is divided into four cases. Figure (5.6 to 5.21) indicates the area control error (ACE (p.u.)), frequency deviation (del F (Hz)) and tie-line error (del P tie (p.u.)) for each simulation case. All the results from Figure (5.6 to 5.21) are summarized in Table (5.3 to 5.6).

In all the cases area control error, frequency deviation and tie-line error from a single load area to each generating area is compared and considered the minimum value of ACE. As ACE is the combination of frequency deviation and tie-line error, so if we take the minimum value of ACE for consideration, it will be possible to select proper feedback connections to load frequency control of BPS.

Case 1: Effect of Load Change at Sirajganj

A load change of 0.1 p.u. in t=2sec. at Sirajganj is considered. The area control error, frequency deviation and tie-line power flow deviation is presented in Figure (5.6 to 5.9). The values of ACE, frequency deviation and tie-line power flow deviation are tabulated in Table 5.3.

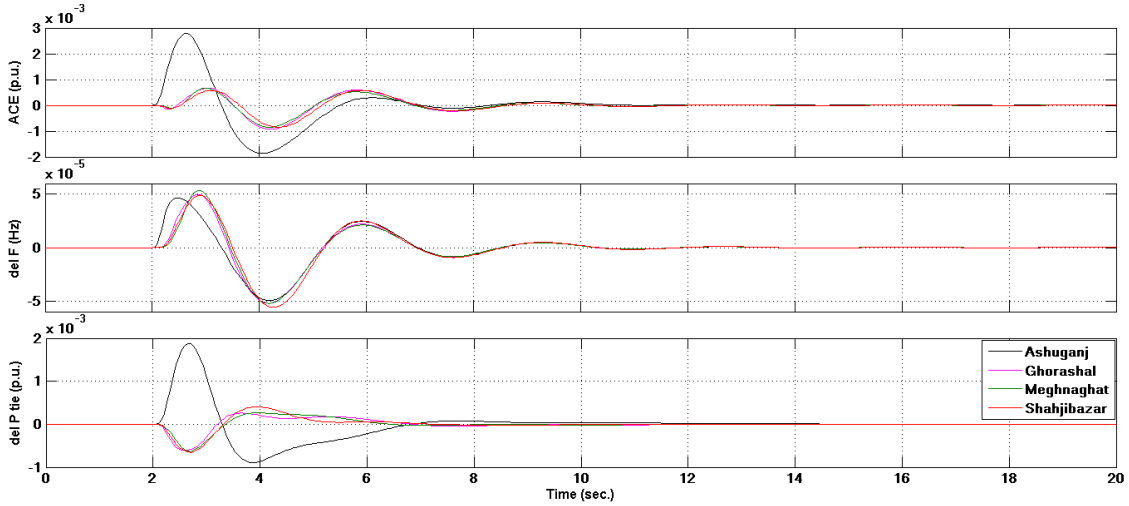

Figure 5.6: Load changes at Sirajganj and feedback to Ashuganj

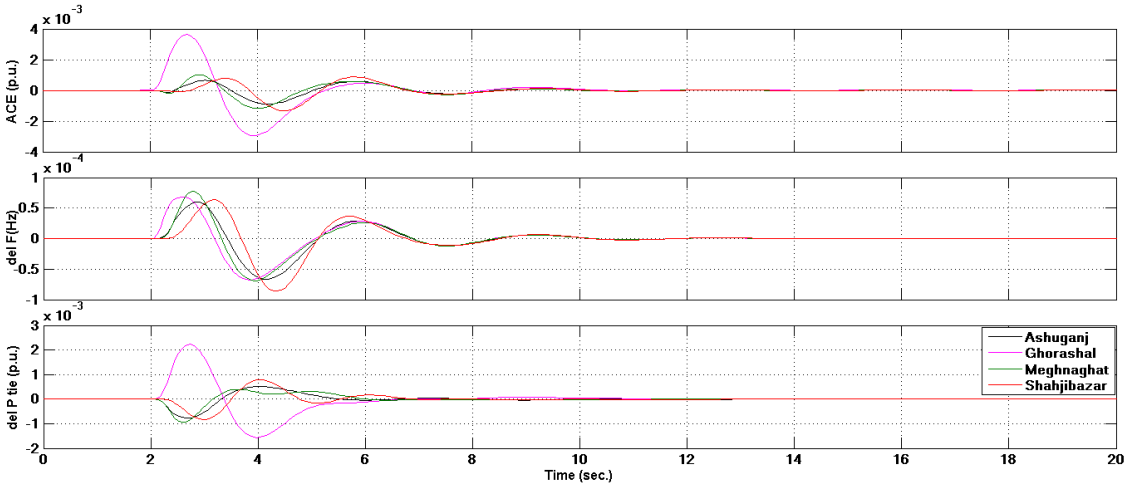

Figure 5.7: Load changes at Sirajganj and feedback to Ghorashal

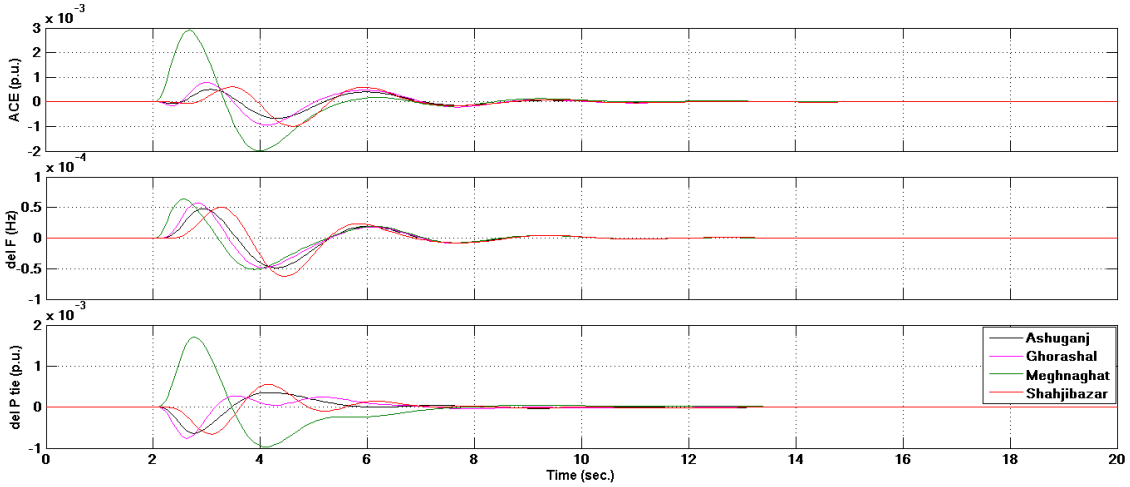

Figure 5.8: Load changes at Sirajganj and feedback to Meghnaghat

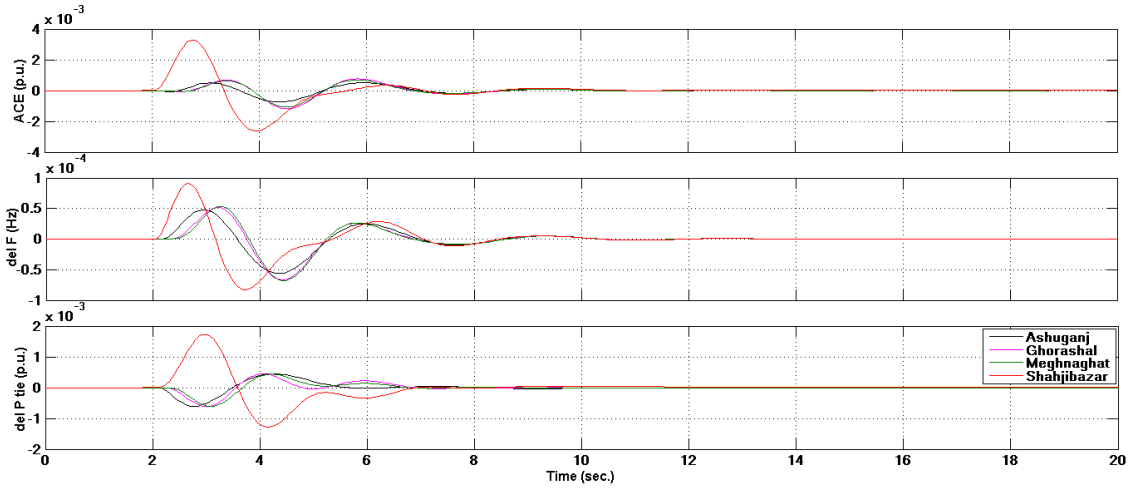

Figure 5.9: Load changes at Sirajganj and feedback to Shahjibazar

Table 5.3: Effect of 0.1 p.u. load change at Sirajganj on various generation rich areas

Feedback from Sirajganj to	**Area Control Error at generation areas**	**Frequency deviation at generation areas**	**Tie-line flow deviation at generation areas**
Ashuganj	2.79e-3	4.9e-5	1.88e-3
Ghorashal	3.61e-3	6.64e-5	2.22e-3
Meghnaghat	2.89e-3	6.38e-5	1.70e-3
Shahjibazar	3.26e-3	9.05e-5	1.72e-3

Findings:

It is seen from Table 5.3 that the lowest ACE is obtained for feedback connection between Sirajganj and Ashuganj. So, feedback from Sirajganj to Ashuganj is proposed to minimize the frequency deviation from the reference value.

Case 2: Effect of Load Change at Kishoreganj

A load change of 0.1 p.u. in t=2sec. at Kishoreganj is considered. The area control error, frequency deviation and tie-line power flow deviation is presented in Figure (5.10 to 5.13). The values of ACE, frequency deviation and tie-line power flow deviation are tabulated in Table 5.4.

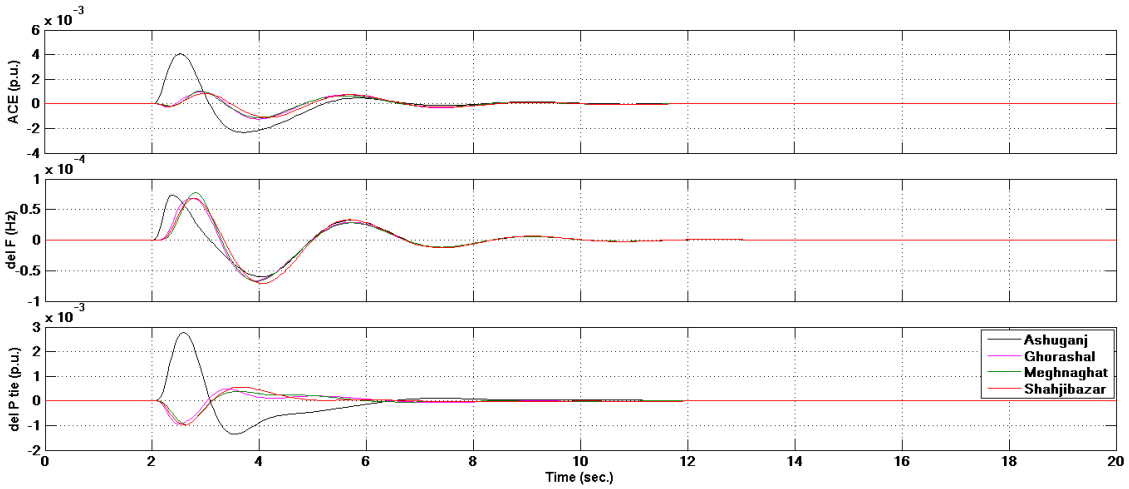

Figure 5.10: Load changes at Kishoreganj and feedback to Ashuganj

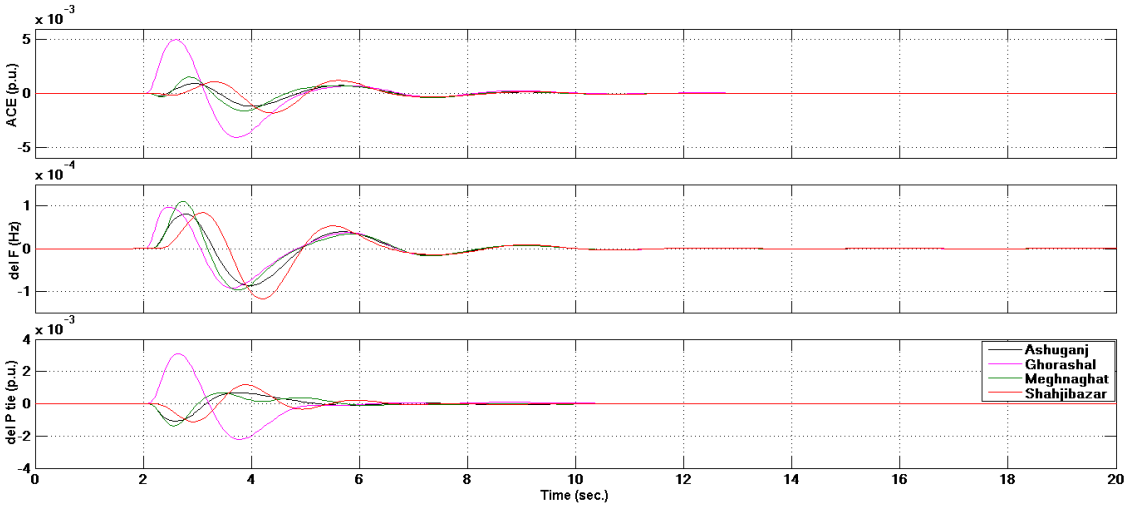

Figure 5.11: Load changes at Kishoreganj and feedback to Ghorashal

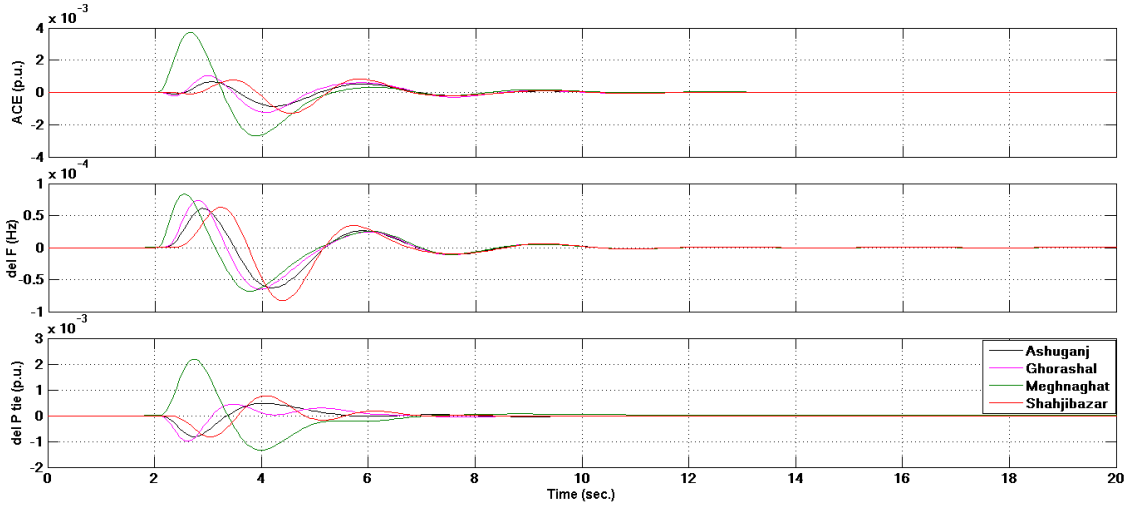

Figure 5.12: Load changes at Kishoreganj and feedback to Meghnaghat

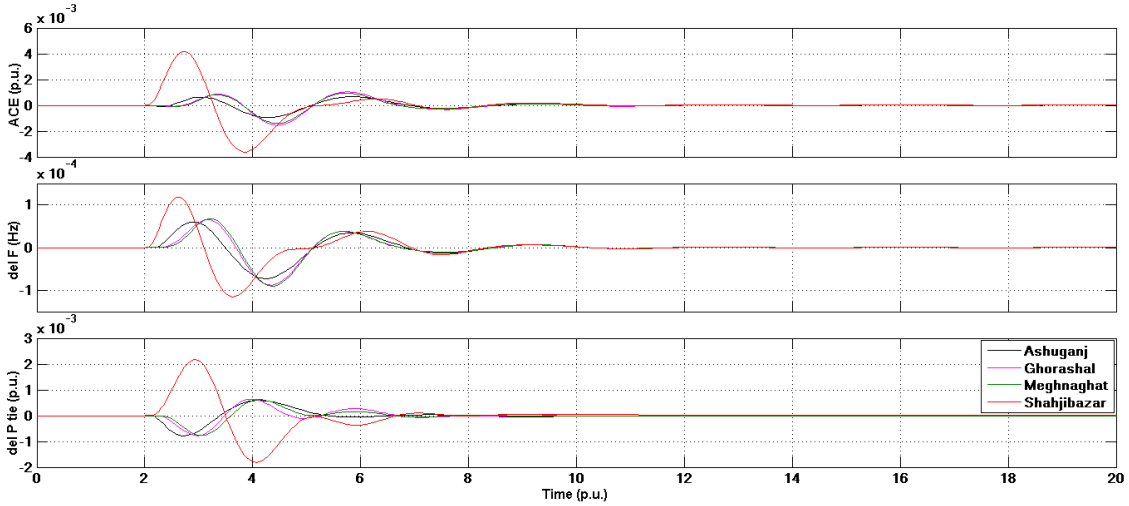

Figure 5.13: Load changes at Kishoreganj and feedback to Shahjibazar

Table 5.4: Effect of 0.1 p.u. load change at Kishoreganj on various generation rich areas

Feedback from Kishoreganj to	**Area Control Error at generation areas**	**Frequency deviation at generation areas**	**Tie-line flow deviation at generation areas**
Ashuganj	4.08e-3	7.38e-5	2.78e-3
Ghorashal	5.01e-3	9.73e-5	3.09e-3
Meghnaghat	3.74e-3	8.36e-5	2.19e-3
Shahjibazar	4.16e-3	1.17e-4	2.17e-3

Findings:

It is seen from Table 5.4 that the lowest ACE is obtained for feedback connection between Kishoreganj and Meghnaghat. So, feedback from Kishoreganj to Meghnaghat is proposed to minimize the frequency deviation from the reference value.

Case 3: Effect of Load Change at Comilla (North)

A load change of 0.1 p.u. in t=2sec. at Comilla (North) is considered. The area control error, frequency deviation and tie-line power flow deviation is presented in Figure (5.14 to 5.17). The values of ACE, frequency deviation and tie-line power flow deviation are tabulated in Table 5.5.

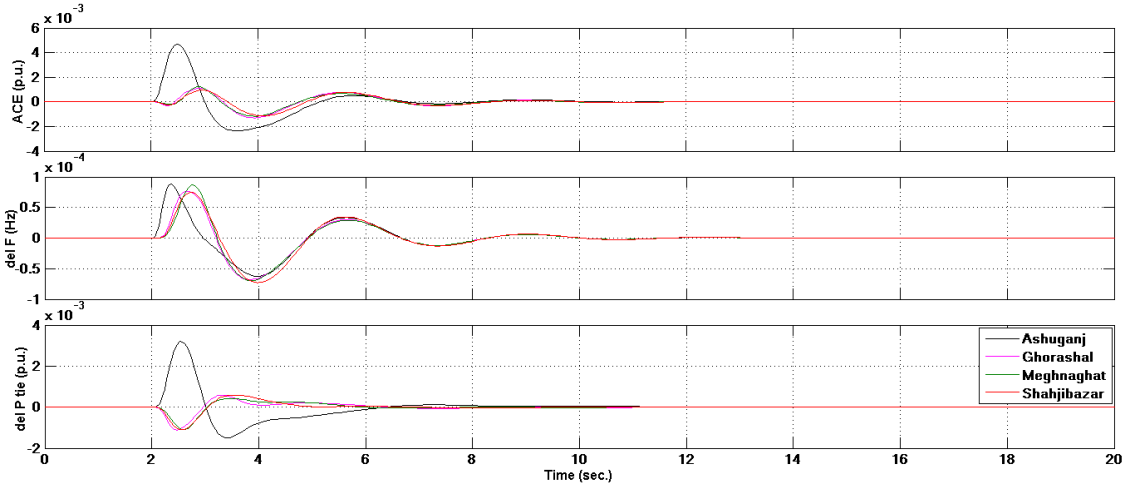

Figure 5.14: Load changes at Comilla (North) and feedback to Ashuganj

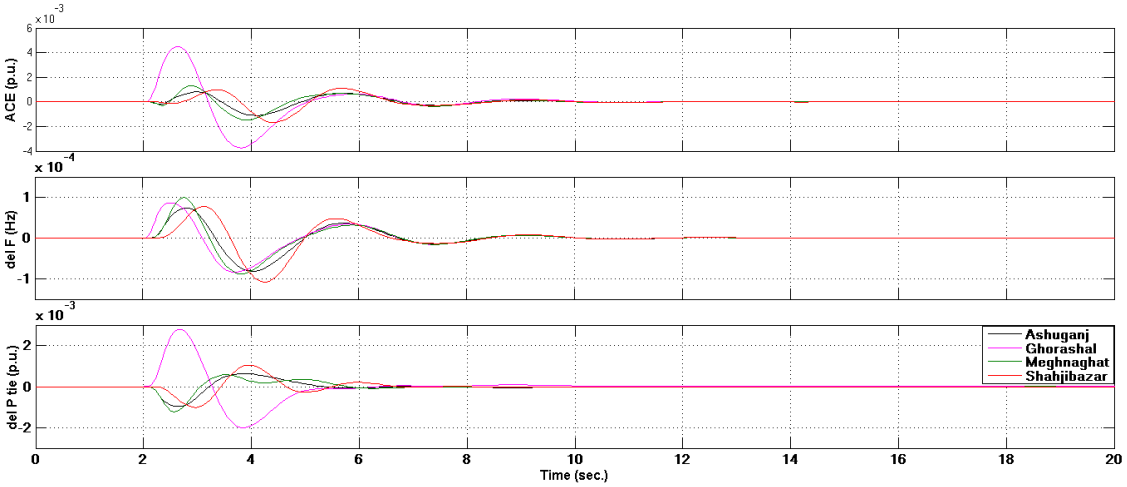

Figure 5.15: Load changes at Comilla (North) and feedback to Ghorashal

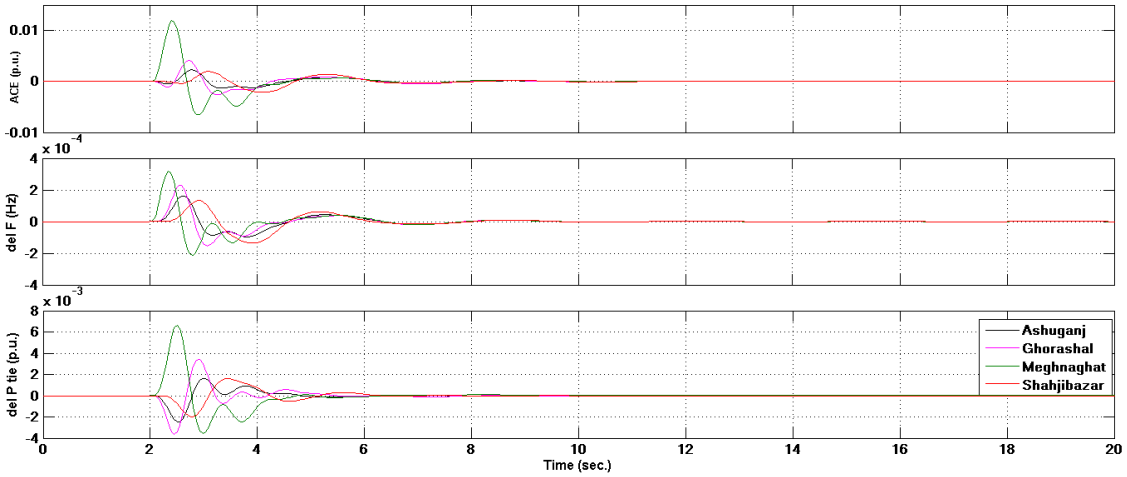

Figure 5.16: Load changes at Comilla (North) and feedback to Meghnaghat

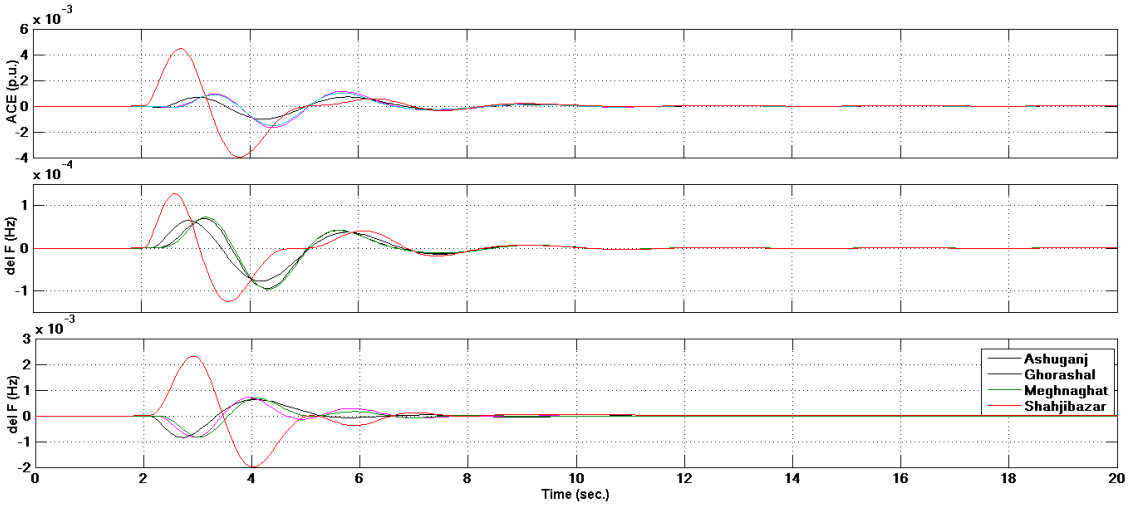

Figure 5.17: Load changes at Comilla (North) and feedback to Shahjibazar

Table 5.5: Effect of 0.1 p.u. load change at Comilla (North) on various generation rich areas

Feedback from Comilla (North) to	**Area Control Error at generation areas**	**Frequency deviation at generation areas**	**Tie-line flow deviation at generation areas**
Ashuganj	4.65e-3	8.83e-5	3.17e-3
Ghorashal	4.49e-3	8.58e-5	2.78e-3
Meghnaghat	12e-3	3.15e-4	6.60e-3
Shahjibazar	4.48e-3	1.27e-4	2.31e-3

Findings:

It is seen from Table 5.5 that the lowest ACE is obtained for feedback connection between Comilla (North) and Shahjibazar. So, feedback from Comilla (North) to Shahjibazar is proposed to minimize the frequency deviation from the reference value.

Case 4: Effect of Load Change at Ishwardi

A load change of 0.1 p.u. in t=2sec. at Ishwardi is considered. The area control error, frequency deviation and tie-line power flow deviation is presented in Figure (5.18 to 5.21). The values of ACE, frequency deviation and tie-line power flow deviation are tabulated in Table 5.6.

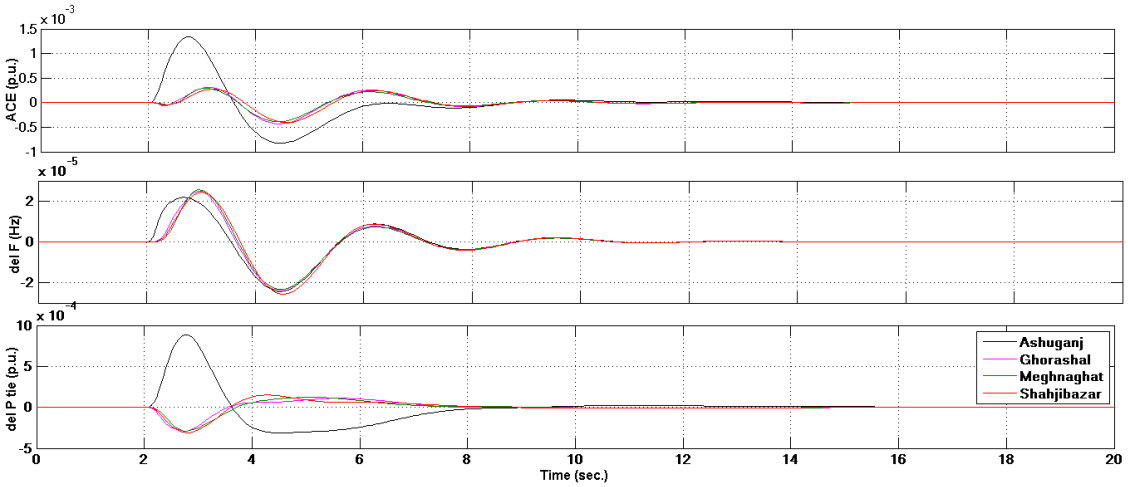

Figure 5.18: Load changes at Ishwardi and feedback to Ashuganj

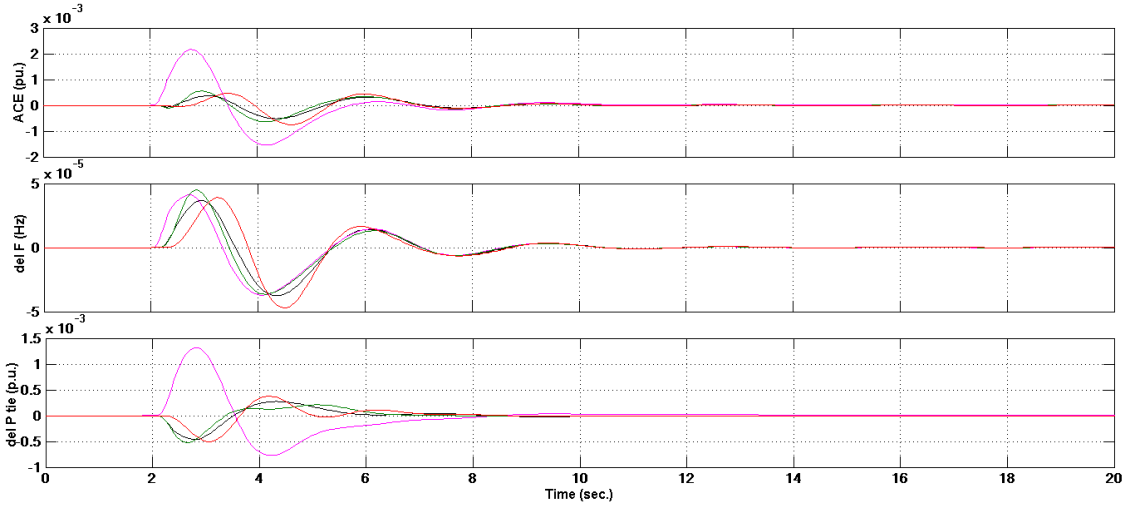

Figure 5.19: Load changes at Ishwardi and feedback to Ghorashal

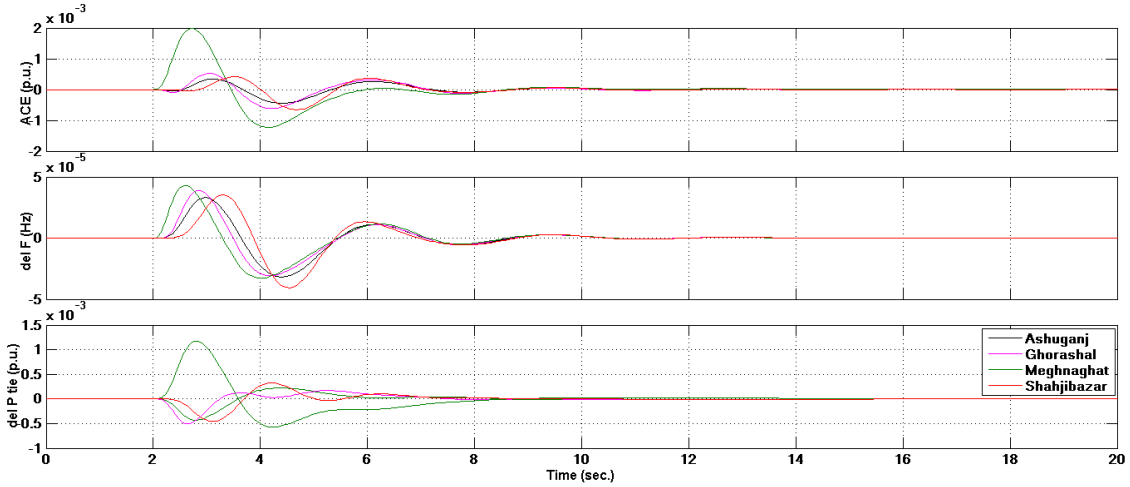

Figure 5.20: Load changes at Ishwardi and feedback to Meghnaghat

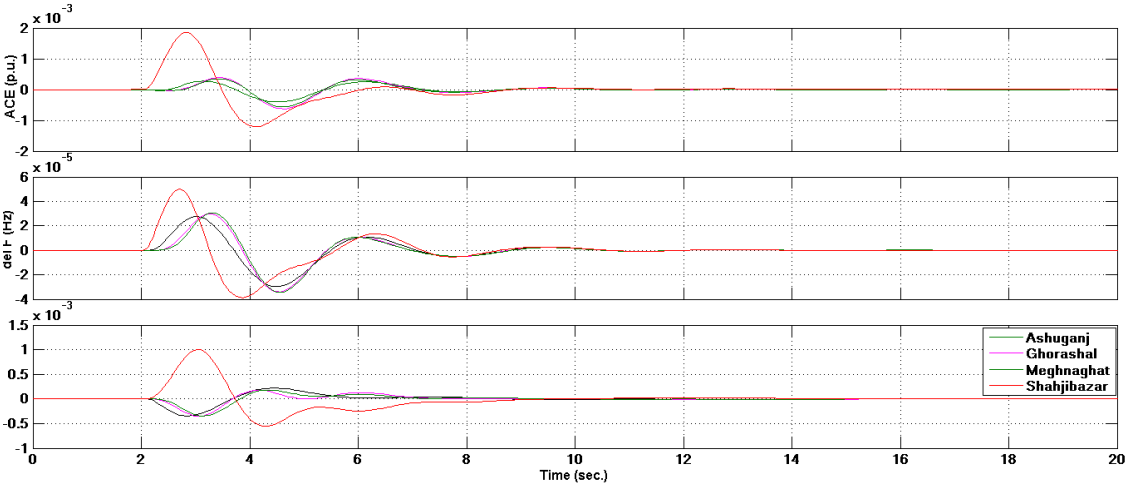

Figure 5.21: Load changes at Ishwardi and feedback to Shahjibazar

Table 5.6: Effect of 0.1 p.u. load change at Ishwardi on various generation rich areas

Feedback from Ishwardi to	**Area Control Error at generation areas**	**Frequency deviation at generation areas**	**Tie-line flow deviation at generation areas**
Ashuganj	1.34e-3	2.43e-5	8.86e-4
Ghorashal	2.16e-3	4.10e-5	1.32e-3
Meghnaghat	1.98e-3	4.30e-5	1.17e-3
Shahjibazar	1.84e-3	5.00e-5	10.00e-4

Findings

It is seen from Table 5.6 that the lowest ACE is obtained for feedback connection between Ishwardi and Ashuganj. So, feedback from Ishwardi to Ashuganj is proposed to minimize the frequency deviation from the reference value.

Proposed Feedback Connections

The ADRC is applied successfully on load frequency control of Bangladesh Power System. From the application of ADRC it is found that the feedback connections from Sirajganj to Ashuganj, Kishoreganj to Meghnaghat, Comilla (North) to Shahjibazar and Ishwardi to Ashuganj is needed to minimize the Area Control error as well as frequency deviation and tie-line error. According to these findings Figure 5.22 can be constructed from Figure 5.2.

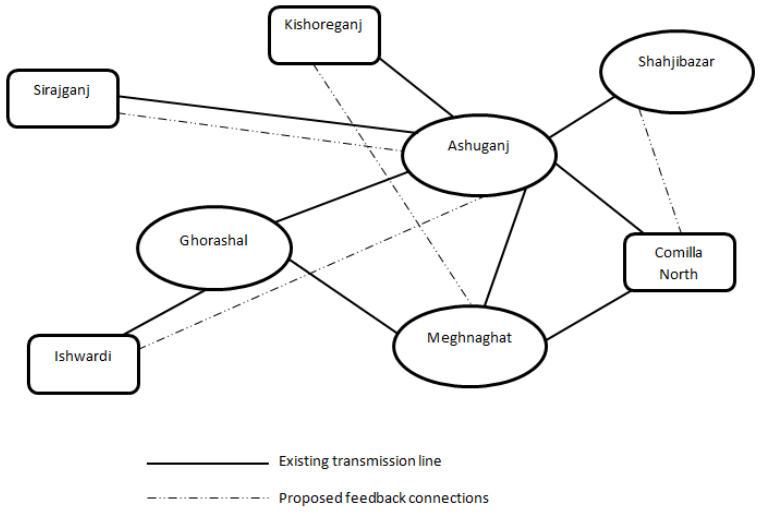

Figure 5.22: Proposed feedback connections from the four load rich areas

In above four cases, all the generators are under ADRC control. An area control error (ACE) for each region is defined based on frequency deviation and change in tie-line power flow in that region. The effect of load change is investigated. Load change information at a particular load bus is directly fed to generators one by one and the resultant deviation in ACE is calculated. Comparing for different feedback connections an optimum feedback connection is selected considering settling time and overshoot for the ACE and for maintaining rated frequency during load changes. And finally, based on the above studies feedback connection from specific load bus to specific generator bus is proposed.

5.2.3 Simulation with Proposed Feedback Connections

Figure 5.23 is modified from Figure 5.3 based on the findings of above simulation results. Feedback connections from Sirajganj and Ishwardi is connected to Ahuganj Power Plant, Kishoreganj is connected to Meghnaghat Power Plant and Comilla (North) is connected to Shahjibazar.

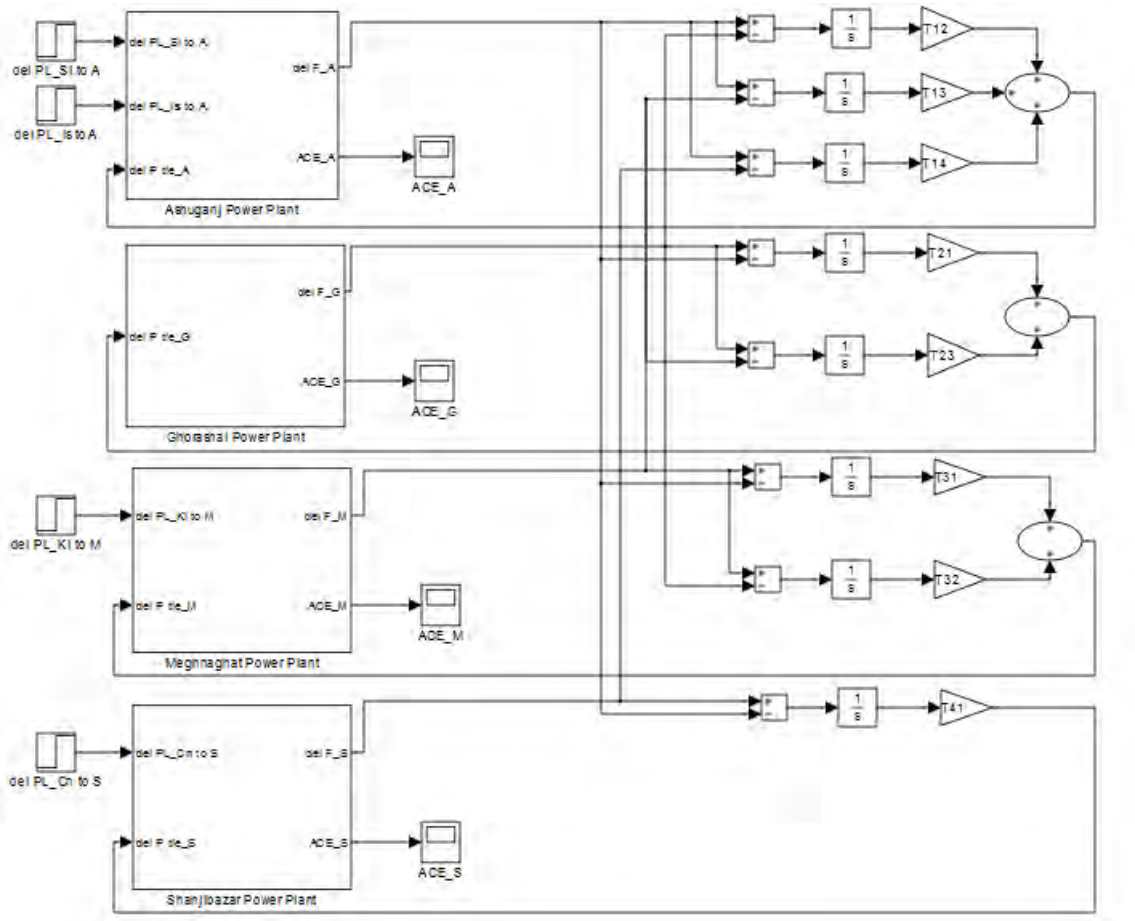

Figure 5.23: Dynamic model of BPS with proposed feedback connections

Figure 5.24 to 5.27 and Table 5.7 shows the ACE, frequency deviation and tie-line error when a 0.1 p.u. load change occurs in Sirajganj, Ishwardi, Kishoreganj and Comilla (North) respectively. From the following figures we observe that if we construct BPS according to the model of Figure 5.23 then the ACE, frequency deviation and tie-line flow error will reduce at a noticeable amount.

Table 5.7: Summary of the errors for proposed feedback connections

Proposed Feedback connections	Area Control Error	Frequency deviation	Tie-line flow deviation
Sirajganj to Ashuganj	2.79e-3	4.9e-5	1.88e-3
Kishoreganj to Meghnaghat	3.74e-3	8.36e-5	2.19e-3
Comilla (North) to Shahjibazar	4.48e-3	1.27e-4	2.31e-3
Ishwardi to Ashuganj	1.34e-3	2.43e-5	8.86e-4

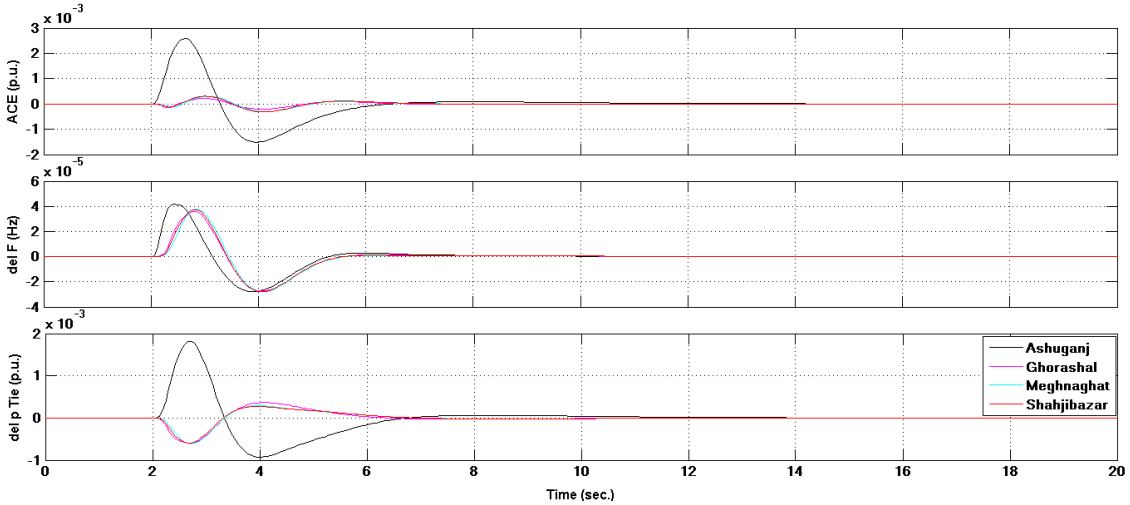

Figure 5.24: Proposed feedback connections from Sirajganj to Ashuganj and its responses

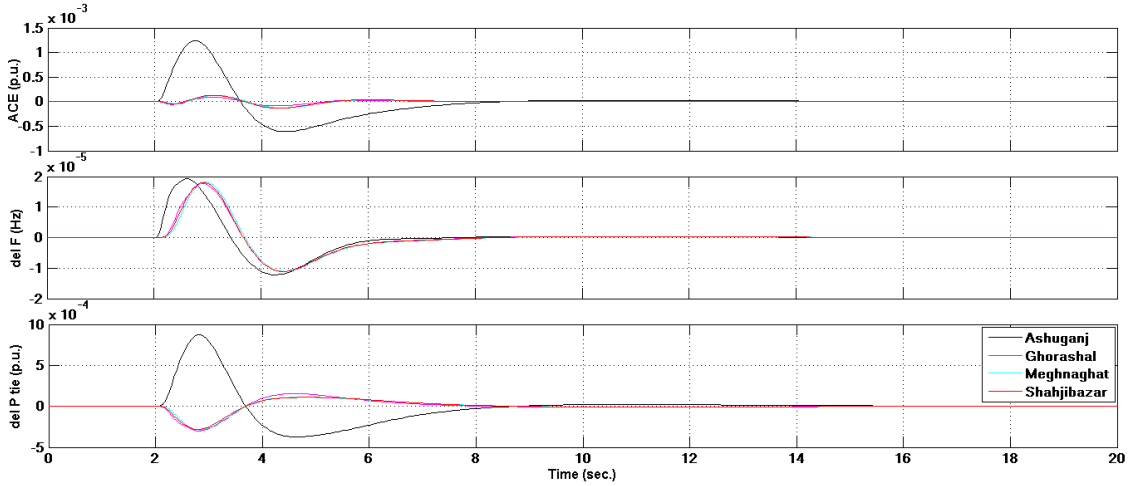

Figure 5.25: Proposed feedback connections from Ishwardi to Ashuganj and its responses

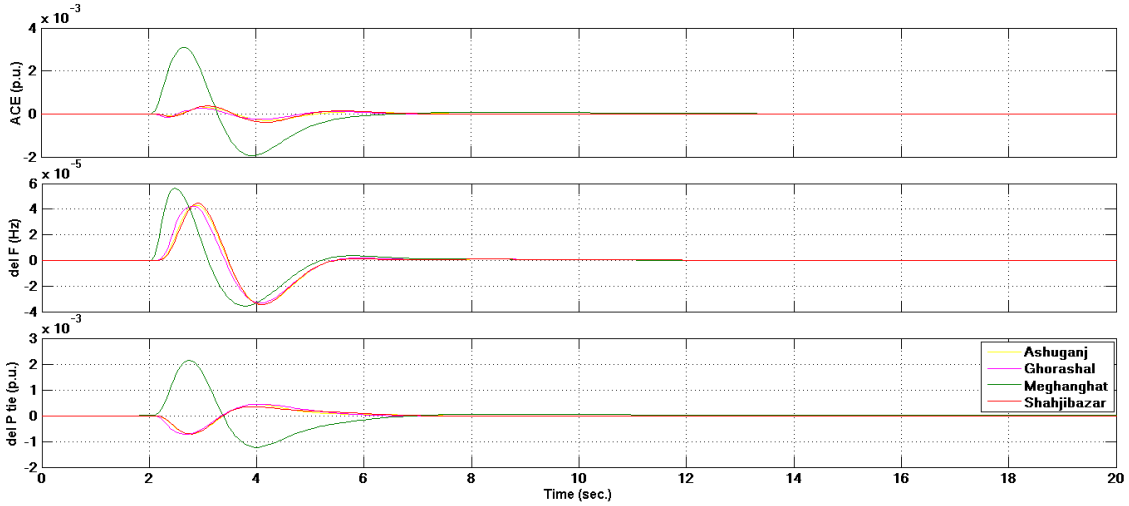

Figure 5.26: Proposed feedback connections from Kishoreganj to Meghnaghat and its responses

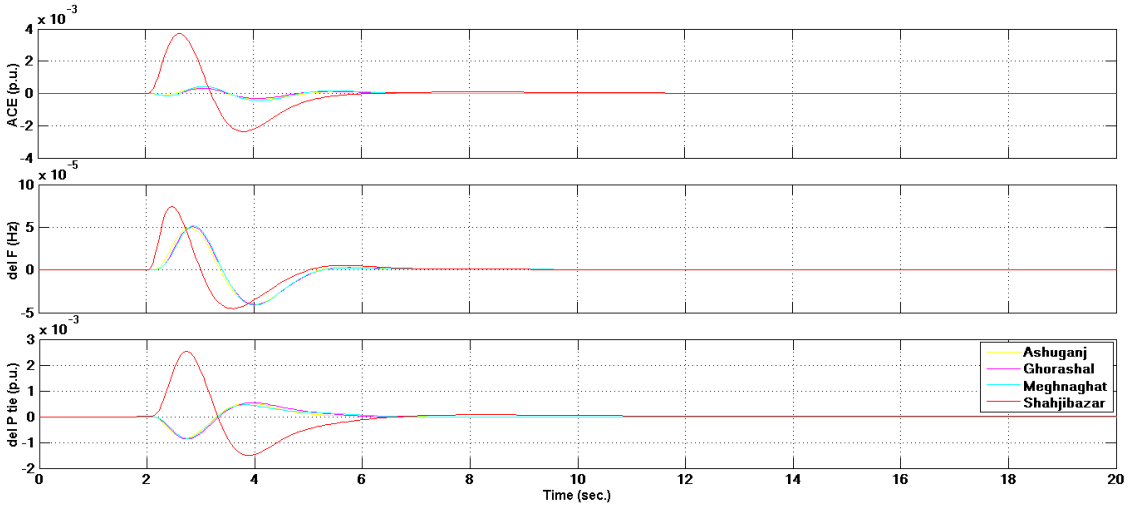

Figure 5.27: Proposed feedback connections from Comilla (North) to Shahjibazar and its responses

Above simulation studies verified the effectiveness of ADRC on the LFC problem of BPS. If we make feedback connections according to the above proposal then ADRC is able to cancel the ACE to satisfy the LFC requirements of maintaining the standard frequency and keeping the tie-line power exchange according to the schedule.

Chapter VI
Conclusion

6.0 Conclusion

In a power system abnormal condition is created through fault or sudden load addition/withdrawn or forced capacity outages or all at a time generates a huge loss to the utility as to the consumers and in Bangladesh it is a common scenario. The loss reaches to an extreme if the abnormal condition leads to a system blackout. Today's power system operations require more careful consideration of all forms of system instability and control problems and to introduce more effective and robust control strategies.

This thesis successfully introduced ADRC for LFC problem of BPS. It proposed an ADRC based decentralized load frequency controller and feedback connections from various load rich areas to generation rich areas to minimize the area control error, frequency errors and tie-line power errors for interconnected power systems of Bangladesh. The simulation results show that the scheme is capable of handling abnormal condition in a power system created by load changes.

The design approaches of ADRC have been explained in detail. Test power systems were established and utilized to test the stability, reliability and robustness of ADRC controlled system in the presences of power load changes and system parameter variations. The three test systems are comparison of performance of ADRC and PID, a two-area two-different-unit power system including reheat and non-reheat units and a large power station. ADRC was simulated on the three types of test systems respectively. The simulation results in time-domain verified the effectiveness of ADRC through successfully regulating the ACE outputs, frequency errors and tie-line power errors in the presences of external disturbance and parameter uncertainties which represents the structural or model uncertainties.

Effectiveness of ADRC on the LFC problem of BPS is verified. If we make feedback connections according to the proposal, ADRC is able to cancel the ACE to satisfy the LFC requirements to maintain the standard frequency and keeping the tie-line power exchange according to the schedule. This work constructed the base to propose a modified feedback connection from four load rich areas of BPS based on ADRC for better load frequency control performance.

ADRC has been applied to multiple areas including MEMS, chemical industry, and aerospace etc. The thesis initiates the successful employment of ADRC technology for Bangladesh Power System.

6.1 Future Work

In the future, the following research on both ADRC and the power system is expected to be conducted.

6.1.1 Improvement of the ADRC

As an increasingly popular practical control method, ADRC has the advantage of requiring little information from the plant and notable robustness against parameter and model uncertainties. But as a novel control technique, it could be improved in the following aspect.

In this work, the designed ADRC can guarantee the fast response of the ACE with small overshoot. However, during the process of simulating ADRC in a power system, the magnitude of the control effort shows a big peak value at the initial stage of the simulation. As we reduce the control effort at the initial stage with a limiter, the control performance will be degraded. In the future, we will need to find a balance between changing the control effort of ADRC and obtaining the optimal ACE response. Through tuning the bandwidths of the ESO and the state feedback controller, we could possibly regulate the relationship between the control effort and the response. But a quantitative method is needed to determine the controller parameters of ADRC. GA and LMI could be applied to tune the parameters in ADRC.

6.1.2 Improvement of the ESO

In real power systems, the large step load disturbances are discontinuous. The linear ESO used in the thesis has the limitation of requiring the disturbance to change smoothly instead of discontinuously. Thus the discontinuous disturbance cannot be accurately estimated by the linear ESO no matter how we tune the bandwidths of the ESO and the state feedback controller. Therefore, in the future, non-linear parts will be included in the ESO or even the whole ADRC to obtain a more accurate approximation of the discontinuous

load disturbance, and hence to make ADRC a more powerful control technique for the power system.

6.1.3 Improvement of the Model and Control of the Power System

For the LFC problem, some of the plant limits such as generation rate constraints and dead bands are disregarded in this thesis. However, in reality, they exist in power system. In the future works, the plant limits in the model of the power system may be included to make the model more practical. Accordingly, the ADRC will also require modification so as to successfully apply it to the new model.

References

[1] P. Kundur, Power System Stability and Control. New York: McGraw-Hill, 1994.

[2] UCTE, *Final report of the investigation committee on the 28 September 2003 blackout in Italy,* Available online at: http://www.ucte.org, 2004.

[3] G. Andersson, P. Donalek, R. Farmer, et al., "Causes of the 2003 major grid blackouts in North America and Europe and recommended means to improve system dynamic performance", *IEEE Transactions on Power Systems,* 20(4), 1922–1928, 2005.

[4] Y. V. Makarov, V. I. Reshetov, V. A. Stroev, et al., *Blackout prevention in the United States, Europe and Russia*, Proc. IEEE, 93(11), 1942–1955, 2005.

[5] M. Sanaye-Pasand, "Security of the Iranian national grid"*, IEEE Power Energy Mag.,* 5(1), pp.31–39, 2007.

[6] H. Bevrani, "Decentralized Robust Load–Frequency Control Synthesis in Restructured Power Systems". *Ph.D. dissertation, Osaka University*, 2004.

[7] N. Jaleeli, D. N. Ewart, and L. H. Fink, "Understanding automatic generation control", *IEEE Trans. Power Syst.,* 7(3), 1106–1112, 1992.

[8] H. Bevrani and T. Hiyama, "Robust load–frequency regulation: A real-time laboratory experiment, Optimal Control Appl. Methods", 28(6), 419–433, 2007.

[9] H. Bevrani and T. Hiyama, "On load–frequency regulation with time delays: Design and real-time implementation," *IEEE Trans. Energy Convers*., in press.

[10] A. Morinec, and F. Villaseca, "Continuous-Mode Automatic Generation Control of a Three-Area Power System," *The 33 rd North American Control Symposium*, pp. 63–70, 2001.

[11] M. Kothari, N. Sinha and M. Rafi, "Automatic Generation Control of an Interconnected Power System under Deregulated Environment," *Power Quality*, vol. 18, pp. 95–102, Jun. 1998.

[12] V. Donde, M. A. Pai, and I. A. Hiskens, "Simulation and Optimization in an AGC System after Deregulation," *IEEE Transactions on Power Systems*, vol. 16, pp. 481–489, Aug. 2001.

[13] M. Aldeen, and R. Sharma, "Robust Detection of Faults in Frequency Control Loops," *IEEE Transactions on Power Systems*, vol. 22, no. 1, pp. 413–422, Feb. 2007.

[14] Y. Moon, H. Ryu, B. Choi, and H. Kook, "Improvement of System Damping by Using the Differential Feedback in the Load Frequency Control," *IEEE Power Engineering Society* 1999 Winter Meeting, vol. 1, pp. 683–688, Feb. 1999.

[15] Y. Moon, H. Ryu, J. Lee, and S. Kim, "Power System Load Frequency Control Using Noise-Tolerable PID Feedback," *IEEE International Symposium on Industrial Electronics*, vol. 3, pp. 1714–1718, Jun. 2001.

[16] Y. Moon, H. Ryu, B. Choi, and B. Cho, "Modified PID Load-Frequency Control with the Consideration of Valve Position Limits," *IEEE Power Engineering Society 1999 Winter Meeting,* vol. 1, pp. 701–706, Feb. 1999.

[17] D. Rerkpreedapong, and A. Feliachi, "PI Gain Scheduler for Load Frequency Control Using Spline Techniques," *The 35 th Southeastern Symposium on System Theory*, pp. 259–263, Mar. 2003.

[18] M. Rahi, and A. Feliachi, "H∞ Robust Decentralized Controller for Nonlinear Power Systems," *The 30th Southeastern Symposium of System Theory,* pp. 268–270, Mar. 1998.

[19] I. Ngamroo, Y. Mitani, and K. Tsuji, "Robust Load Frequency Control by Solid-State Phase Shifter Based on H∞ Control Design," *IEEE Power Engineering Society 1999 Winter Meeting,* vol. 1, pp. 725–730, Feb. 1999.

[20] A. Bensenouci, and A. Ghany, "Mixed H∞ /H2 with Pole-Placement Design of Robust LMI-Based Output Feedback Controllers for Multi-Area Load Frequency Control," *Proceedings of The International Conference on Computer as a Tool*, pp. 1561–1566, Sep. 2007.

[21] D. Rerkpreedapong, and A. Feliachi, "Decentralized H_∞ Load Frequency Control Using LMI Control Toolbox," *The 2003 International Symposium on Circuits and Systems,* vol. 3, no. 25–28, pp. 411–414, May 2003.

[22] A. Paradkar, A. Davari, and A. Feliachi, "Disturbance Accommodation Control versus Conventional Control, in LFC of a Two Area Distribution System in a Deregulated Environment," *The 35 th Southeastern Symposium on System Theory*, pp. 98–102, Mar. 2003.

[23] Y. Moon, H. Ryu, B. Kim, and K. Song, "Optimal Tracking Approach to Load Frequency Control in Power Systems," *IEEE Power Engineering Society 2000 Winter Meeting,* vol. 2, pp. 1371–1376, Jan. 2000.

[24] L. Kong and L. Xiao, "A New Model Predictive Control Scheme-Based Load-Frequency Control," *Proceedings of IEEE International Conference on Control and Automation,* pp. 2514–2518, Jun. 2007.

[25] B. Bakken, and O. Grande, "Automatic Generation Control in a Deregulated Power System," *IEEE Transactions on Power Systems,* vol. 13, no. 4, pp. 1401–1406, Nov. 1998.

[26] Ibraheem, P. Kumar and D. Kothari, "Recent Philosophies of Automatic Generation Control Strategies in Power Systems," *IEEE Transactions on Power Systems, vol.* 20, no. 1, pp. 346–357, Feb. 2005.

[27] T. Hiyama, S. Koga and Y. Yoshimuta, "Fuzzy Logic Based Multi-Functional Load Frequency Control," *IEEE Power Engineering Society* 2000 Winter Meeting, vol. 2, pp. 921–926, Jan. 2000.

[28] K. Yukita, Y. Goto, K. Mizuno, T. Miyafuji, K. Ichiyanagi, and Y. Mizutani, "Study of Load Frequency Control using Fuzzy Theory by Combined Cycle Power Plant," *IEEE Power Engineering Society* 2000 Winter Meeting, vol. 1, pp. 422–427, Jan. 2000.

[29] H. Mohamed, L. Hassan, M. Moghavvemi, and S. Yang, "Load Frequency Controller Design for Iraqi National Super Grid System Using Fuzzy Logic Controller," *SICE Annual Conference*, pp. 227–232, Aug. 2008.

[30] D. Rerkpreedapong, A. Hasanovic, and A. Feliachi, "Robust Load Frequency Control Using Genetic Algorithms and Linear Matrix Inequalities," *IEEE Transactions on Power Systems,* vol. 18, no. 2, pp. 855–861, May 2003.

[31] S. Ohba, H. Ohnishi, and S. Iwamoto, "An Advanced LFC Design Considering Parameter Uncertainties in Power Systems," *Proceedings of IEEE conference on Power Symposium,* pp. 630–635, Sep. 2007.

[32] Z. Gao, Y. Huang, and J. Han, "An Alternative Paradigm for Control System Design," *Proceedings of IEEE Conference on Decision and Control*, vol. 5, no. 4–7, pp. 4578–4585, Dec. 2001.

[33] Z. Gao, "Active Disturbance Rejection Control: A Paradigm Shift in Feedback Control System Design," Proceedings *of American Control Conference*, pp. 2399–2405, Jun. 2006.

[34] Z. Gao, "Scaling and Parameterization Based Controller Tuning," *Proceedings of American Control Conference, vo*l. 6, no. 4–6, pp. 4989–4996, June 2003.

[35] R. Miklosovic, and Z. Gao, "A Robust Two-Degree-of-Freedom Control Design Technique and Its Practical Application," *The 39th IAS Annual Meeting, Industry Applications Conference,* vol. 3, pp. 1495–1502, Oct. 2004.

[36] G. Tian, and Z. Gao, "Frequency Response Analysis of Active Disturbance Rejection Based Control System," *Proceedings of IEEE International Conference on Control Applications*, pp. 1595–1599, Oct. 2007.

[37] B. Sun, and Z. Gao, "A DSP-Based Active Disturbance Rejection Control Design for a 1-kW H-bridge DC-DC Power Converter," *IEEE Transactions on Industrial Electronics*, vol. 52, no.5, pp. 1271–1277, Oct. 2005.

[38] Z. Chen, Q. Zheng, and Z. Gao, "Active Disturbance Rejection Control of Chemical Processes," *Proceedings of IEEE International Conference on Control Applications*, pp. 855–861, Oct. 2007.

[39] W. Zhou, and Z. Gao, "An Active Disturbance Rejection Approach to Tension and Velocity Regulations in Web Processing Lines," *IEEE International Conference on Control Applications*, pp. 842–848, Oct. 2007.

[40] L. Dong, Q. Zheng, and Z. Gao, "A Novel Oscillation Controller for Vibrational MEMS Gyroscopes," *Proceedings of American Control Conference*, pp. 3204–3209, Jul. 2007.

[41] L. Dong, and D. Avanesian, "Drive-mode Control for Vibrational MEMS Gyroscopes," *IEEE Transactions on Industrial Electronics,* vol. 56, no. 4, pp. 956–963, 2009.

[42] L. Dong, Q. Zheng, and Z. Gao, "On Control System Design for the Conventional Mode of Operation of Vibrational Gyroscopes," *IEEE Sensors Journal*, vol. 8, no. 11, pp. 1871–1878, Nov. 2008.

[43] Y. Zhang, L. Dong and Z. Gao, "Load Frequency Control for Multiple-Area Power Systems", to appear in *Proceedings of American Control Conference*, St. Louis, Mo, Jul. 2009.

[44] J. Edwards, "Modeling and Feedback Control of a MEMS Electrostatic Actuator", *Master's Thesis, Department of Electrical and Computer Engineering, Cleveland State University*, May 2009.

[45] Q. Zheng, L. Dong, D. Lee, and Z. Gao, "Active Disturbance Rejection Control and Implementation for MEMS Gyroscopes," to appear in *IEEE Transactions on Control System Technology*, 2009.

[46] Ahsan, M. Q., Chowdhury, A. H., Ahmed, S. S., Bhuyan, I. Hassan, Haque, M. A., and Rahman, H. "Technique to Develop Auto Load Shedding and Islanding Scheme to Prevent Power System Blackout", IEEE Transactions on Power Systems, vol. 27, no.1, February 2012, pp.198-205.

Annexure A

ADRC and Simulation Parameters

Table A-1: System Parameters for Figure 4.1

M_1 (p.u. sec.)*	10 ± 20%
D_1 (p.u./Hz)	1 ± 20%
Tch_1 (sec.)	0.3 ± 20%
Tg_1 (sec.)	0.1 ± 20%
R_1 (Hz/p.u.)	0.05 ∓ 20%
T_1 (p.u./rad.)	22.6 ± 20%

*: p.u. represents per unit.

Table A-2: ADRC and PID Parameters for Figure 4.1

ADRC		**PID**	
Order of ESO	3	Proportional	o
ω_c	4	Integral	-0.293980028198636
ω_o	20	Derivative	0
b	70.0		

Table A-3: System parameters for Figure 4.5

Non-reheat		**Reheat**	
M_1 (p.u. sec.)*	10 ± 20%	M_2 (p.u. sec.)	10.0
D_1 (p.u./Hz)	1 ± 20%	D_2 (p.u./Hz)	1.0
Tch_1 (sec.)	0.3 ± 20%	Tch_2 (sec.)	0.3
Tg_1 (sec.)	0.1 ± 20%	Fhp	0.3
R_1 (Hz/p.u.)	0.05 ∓ 20%	Trh (sec.)	7.0
T_1 (p.u./rad.)	22.6 ± 20%	Tg_2 (sec.)	0.2
		R_2 (Hz/p.u.)	0.05
		T_2 (p.u./rad.)	22.6

Table A-4: ADRC parameters for Figure 4.5

	Order of ESO	ω_c	ω_o	b
Area 1	3	4	20	70.0
Area 2	3	4	20	10.5

Table A-5: System parameters for Figure 4.12

Parameters	**Generating units**							
MVA base (1000 MW)	**1**	**2**	**3**	**4**	**5**	**6**	**7**	**8**
D (p.u./Hz)	0.0150	0.0140	0.0150	0.0160	0.0140	0.0140	0.0150	0.0160
M (p.u. sec)	0.1667	0.1200	0.2000	0.2017	0.1500	0.1960	0.1247	0.1667
Tch (sec.)	0.4	0.36	0.42	0.44	0.32	0.40	0.30	0.40
Tg (sec.)	0.08	0.06	0.07	0.06	0.06	0.08	0.07	0.07
R (Hz/ p.u.)	3.00	3.00	3.30	2.7273	2.6667	2.50	2.8235	3.00
B (p.u./Hz)	0.3483	0.3473	0.3180	0.3827	0.3890	0.4140	0.3692	0.3493
Fhp			0.3	0.3	0.3			
Trh (sec.)			7.0	7.0	7.0			
T (p.u./rad.)	0.2	0.12	0.25	0.2	0.12	0.25	0.2	0.12

Table A-6: ADRC parameters for Figure 4.12

	Order of ESO	ω_c	ω_o	b
Unit 1	3	4	20	70.0
Unit 2	3	4	20	70.5
Unit 3	3	4	20	10.5
Unit 4	3	4	20	10.5
Unit 5	3	4	20	10.5
Unit 6	3	4	20	70.0
Unit 7	3	4	20	70.0
Unit 8	3	4	20	70.0

Table A-7: System parameters for Figure 5.3

Parameters	**Generation rich area**				**Load rich area**			
MVA base (1000 MW)	**Ashuganj**	**Ghorasal**	**Meghnaghat**	**Sylhet**	**Sirajganj**	**Kishoreganj**	**Comilla North**	**Ishwardi**
D (p.u./Hz)	1	1	1	1	1	1	1	1
M (p.u. sec)	10	10	10	10	10	10	10	10
Tch (sec.)	0.3	0.3	0.3	0.3	0.3	0.3	0.3	0.3
Tg (sec.)	0.2	0.2	0.2	0.2	0.2	0.2	0.2	0.2
R (Hz/ p.u.)	0.05	0.05	0.05	0.05	0.05	0.05	0.05	0.05
Fhp	0.3	0.3	0.3	0.3	0.3	0.3	0.3	0.3
Trh (sec.)	7	7	7	7	7	7	7	7
T (p.u. /rad.)								
T12=77.23			T51=29.14		T53=17.19			
T13=31.87			T61=52.81		T63=23.75			
T14=52.81			T71=66.23		T73=169.80			
T21=77.23			T81=11.03		T83=10.9302			
T23=72.41			T52=25.60		T54=18.78			
T31=31.87			T62=42.23		T64=26.405			
T32=72.41			T72=35.66		T74=29.38			
T41=52.81			T82=12.87		T84=9.27			

Table A-8: ADRC parameters for Figure 5.3

	Order of ESO	ω_c	ω_o	b
Asuganj	3	4	20	70.0
Ghorashal	3	4	20	70.0
Meghnaghat	3	4	20	70.0
Sylhet	3	4	20	70.0
Sirajganj	3	4	20	10.5
Kishoreganj	3	4	20	10.5
Comilla North	3	4	20	10.5
Ishwardi	3	4	20	10.5